ERDC/GSL TR-18-31

Geotechnical and Structures Laboratory

US Army Corps
of Engineers®
Engineer Research and
Development Center

ERDC
ENGINEER RESEARCH & DEVELOPMENT CENTER

Mechanical Behavior of Cor-Tuf Ultra-High Performance Concrete Considering Aggregate and Paste Effects

Isaac L. Howard, Ashley Carey, Megan Burcham,
Dylan A. Scott, Jameson D. Shannon, Robert D. Moser,
and Mark F. Horstemeyer

October 2018

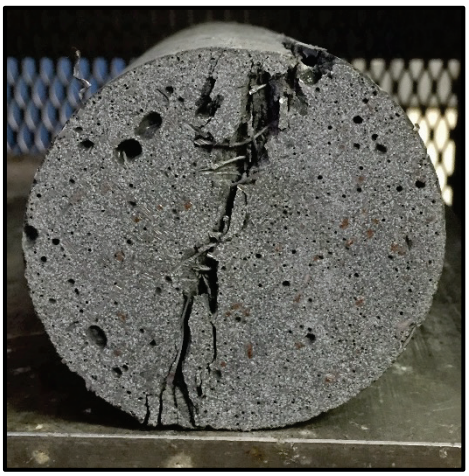

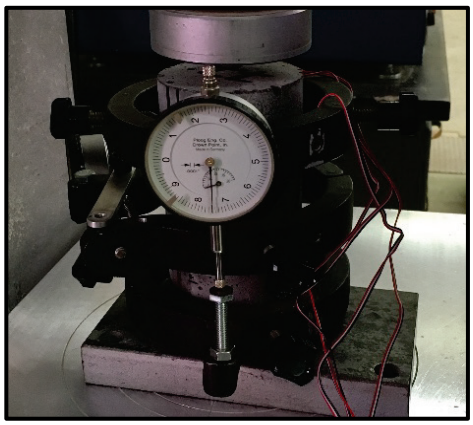

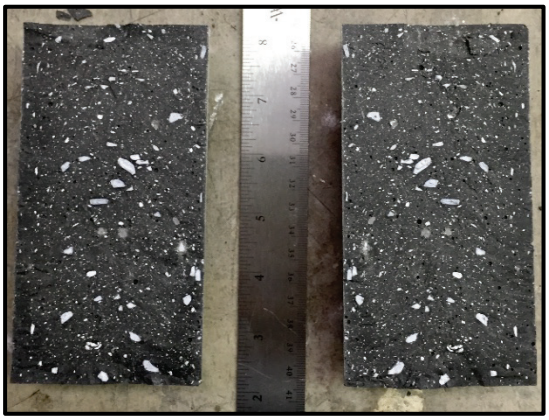

Approved for public release; distribution is unlimited.

The U.S. Army Engineer Research and Development Center (ERDC) solves the nation's toughest engineering and environmental challenges. ERDC develops innovative solutions in civil and military engineering, geospatial sciences, water resources, and environmental sciences for the Army, the Department of Defense, civilian agencies, and our nation's public good. Find out more at www.erdc.usace.army.mil.

To search for other technical reports published by ERDC, visit the ERDC online library at http://acwc.sdp.sirsi.net/client/default.

ERDC/GSL TR-18-31
October 2018

Mechanical Behavior of Cor-Tuf Ultra-High Performance Concrete Considering Aggregate and Paste Effects

Dylan Scott, Robert Moser, and Jameson D. Shannon

Geotechnical and Structures Laboratory
Concrete Materials Branch
U.S. Army Engineer Research and Development Center (ERDC)
3909 Halls Ferry Road
Vicksburg, MS 39180

Isaac L. Howard

Center for Advanced Vehicular Systems and
Civil and Environmental Engineering Department
Mississippi State University
200 Research Boulevard
Starkville, MS 39759

Ashley Carey, Megan Burcham, and Mark F. Horstemeyer

Center for Advanced Vehicular Systems and
Mechanical Engineering Department
Mississippi State University
200 Research Boulevard
Starkville, MS 39759

Final report

Approved for public release; distribution is unlimited.

Prepared for U.S. Army Corps of Engineers
Washington, DC 20314-1000

Under ERS, IVPPED, and WD63 multiscale cements contracts

Abstract

This research primarily focused on properties from varying the constituents that make up ultra-high performance concrete (UHPC) with the ultimate goal to enable improved characterization and modeling of this material. Several variations of UHPC were made to see the differences in properties as a function of constituents. Compressive strength, elastic modulus, and tensile strength were measured at low loading rates. Fundamental test methods were used for most experiments with a smaller subset of tests with strain gages and imaging techniques. This report is intended primarily to document these experiments and the collected data. Specific conclusions are avoided herein, as the intent is to use these data in future efforts that will be more appropriate to draw more meaningful conclusions about ways to better model and ultimately improve UHPC.

DISCLAIMER: The contents of this report are not to be used for advertising, publication, or promotional purposes. Citation of trade names does not constitute an official endorsement or approval of the use of such commercial products. All product names and trademarks cited are the property of their respective owners. The findings of this report are not to be construed as an official Department of the Army position unless so designated by other authorized documents.

DESTROY THIS REPORT WHEN NO LONGER NEEDED. DO NOT RETURN IT TO THE ORIGINATOR.

Contents

Figures and Tables

Figures

Tables

Preface

This study was conducted for USACE through a collaboration between the U.S. Army Engineer Research and Development Center (ERDC) and the Mississippi State University (MSU) Center for Advanced Vehicular Systems (CAVS). The contents of this report were supported by three research contracts: “Engineered Resilient Systems” (ERS), “Integrated Virtual Prototyping for Product Engineering and Design” (IVPPED), and “Engineering Work Directive 0063” (WD63). IVPPED was sponsored by ERDC under Cooperative Agreement Number W56HZV-17-C-0095. The technical monitor for IVPPED was Ms. Vernessa Noye. Dr. Roger L. King was the CAVS Director and Principal Investigator for most activities documented in this report, and Dr. Clay Walden assumed the responsibility of CAVS Director near the end of this report’s activities.

The work was performed by the Concrete and Materials Branch (CMB) of the Engineering Systems and Materials Division (ESMD), ERDC Geotechnical and Structures Laboratory (GSL). At the time of publication, Mr. Christopher Moore was Chief, CMB; Dr. Gordon W. McMahon was Chief, ESMD; and Dr. Michael Sharp was Technical Director for Civil Works Infrastructure. The Deputy Director of ERDC-GSL was Dr. William P. Grogan, and the Director was Mr. Bartley P. Durst.

COL Ivan P. Beckman was the Commander of ERDC, and Dr. David W. Pittman was the Director.

Unit Conversion Factors

Multiply	By	To Obtain
degrees Fahrenheit	(F-32)/1.8	degrees Celsius
inches	0.0254	meters
pounds (force) per square inch	6.894757	kilopascals
pounds (mass)	0.45359237	kilograms
pounds (mass) per cubic inch	2.757990 E+04	kilograms per cubic meter
square inches	6.4516 E-04	square meters

1 Introduction

1.1 Background

In recent years, ultra-high performance concrete (UHPC) has been studied from many perspectives including flexural and tensile properties (Roth 2008), fiber size and shape (Scott et al. 2015), and nanomechanical analysis of calcium-silicate-hydrate (Chandler et al. 2012). However, studying effects of individual constituents and, for example, how they fit into a multiscale numerical modeling framework have not been as widely studied.

UHPC is usually composed of five to eight individual materials with varying sizes and length scales. Typical materials are in one of five categories: water, cementitious material, admixture, fiber, or fine aggregate. Coarse aggregates are not incorporated into UHPC to avoid relatively large failure planes that can occur when large aggregates have a weak plane within them. This problem is lessened when only fine aggregates, such as sand, are incorporated. UHPC makes use of water reducing admixtures so less water is needed for equal fluidity. With less water, cement paste (CP) is stronger after hydration. Fibers, typically steel, but in some cases polymeric are added for improved ductility.

UHPC is not used nearly as often as traditional concrete, but it does have several applications. This report does not contain a comprehensive literature review as its primary purpose is to document a series of fundamental experiments that are intended to be utilized in companion efforts. A state-of-the-art report on UHPC and its history is available in Green et al. (2014).

1.2 Objectives

The data collected and documented in this report aim to further the UHPC knowledge base for improved characterization and are also intended for use in numerical modeling. A laboratory test program undertaken to measure fundamental UHPC properties, beginning with individual constituents, is documented here. The scope of this effort focuses mainly on experimental efforts with Cor-Tuf UHPC, which was developed by

ERDC. An ultimate goal is for this report to be used alongside additional data in high-performance computing environments.

1.3 Scope

This effort investigated properties at low load rates and with no specimen confinement, which allowed more specimen replication, albeit producing less sophisticated measurements. The goal of this portion of a larger multiscale cementitious materials program was to understand the effects of individual UHPC components. Once fundamental understanding of individual components, proportioning, and their interfacial behavior is better understood, mathematical relations to improve the state-of-the-art in numerical modeling of UHPC should be more feasible.

Four types of specimens were evaluated: CP, mortar (M), fiber reinforced paste (FRP), and UHPC. CP has no aggregates or fibers, M has no fibers, FRP has no aggregates, and UHPC has all ingredients. A systematic evaluation containing these specimen types produced from the same ingredients (sometimes with varying proportions) is not commonplace and is the main contribution of this effort. Specimens of these varying types are intended to isolate contributions/behaviors of the three primary ingredient classifications (paste, aggregates, and fibers) that can be benchmarked to these materials combined (i.e., Cor-Tuf UHPC).

This report represents work performed beginning in 2013 under three programs: Engineered Resilient Systems (ERS), Integrated Virtual Prototyping for Product Engineering and Design (IVPPED), and Engineering Work Directive 0063 (WD63). Earlier efforts within ERS were largely conceptual, with emphasis on how laboratory measurements of individual constituents might be able to support high performance computing based modeling and simulation investigations focused on concrete multi-scale modeling. Later, specimens began to be prepared, cured, and tested (mostly within IVPPED). Thereafter, data analysis occurred mostly within WD63. Report assembly occurred progressively throughout the work.

1.4 Symbols and acronyms

The following symbols and acronyms are used throughout the report.

ACI – American Concrete Institute

API – American Petroleum Institute

ASTM – American Society for Testing and Materials

C_{469} – elastic modulus constant found from the relationship of compressive strength to elastic modulus

CAVS – Center for Advanced Vehicular Systems

CMRC – Construction Materials and Research Center

COV – coefficient of variation, standard deviation divided by mean

CP – cement paste

CP-0.11 – cement paste with a water to cementitious material ratio of 0.11

CP-0.15 – cement paste with a water to cementitious material ratio of 0.15

CP-0.26 – cement paste with a water to cementitious material ratio of 0.26

CT – computed topography

D – diameter

E – elastic modulus

E_{469} – elastic modulus from ASTM C469

E_{SG} – elastic modulus measured by using strain gages to measure strain

ERDC – U.S. Army Engineer Research and Development Center

ERS – Engineered Resilient Systems

FRP – fiber reinforced paste

FRP-0.11 – fiber reinforced paste with fibers to cementitious material ratio of 0.11

FRP-0.17 – fiber reinforced paste with fibers to cementitious material ratio of 0.17

FRP-0.23 – fiber reinforced paste with fibers to cementitious material ratio of 0.23

HPC – High Performance Computing

HSR – High Sulfate Resistance

IVPPED – Integrated Virtual Prototyping for Product Engineering and Design

M – mortar

M-0.47 – mortar with a fine aggregate to cementitious material ratio of 0.47

M-0.56 – mortar with a fine aggregate to cementitious material ratio of 0.56

M-0.65 – mortar with a fine aggregate to cementitious material ratio of 0.65

MPa – megapascal

MSU – Mississippi State University

N - Newton

^{o}C-d – measure of maturity that is degree Celsius * days

P – load

RVE – Representative Volume Element

SEM – Scanning Electron Microscope

SG – strain gage

St – tensile strength

UHPC – Ultra-high performance concrete

V_a – volume of air

V_{am} – volume of admixture

V_c – volume of cement

V_{noair} – volume of the specimen if there were no air

V_s – volume of sand

V_{sf} – volume of silica fume

V_{sfl} – volume of silica flour

V_{Total} – total volume

V_w – volume of water

WD63 – Engineering Work Directive 0063

a – air

am – admixture

c – cement

cm – cementitious material (class H cement and silica fume)

d_{dial} – displacement of the compressometer dial

f – fibers

f/cm ratio – ratio of fibers to cementitious materials

fa – fine aggregate (silica flour and silica sand)

fa/cm – ratio of fine aggregate to cementitious materials

fc – compressive strength

l – length

l/D – aspect ratio

$m_{b\text{-}per}$ – batching mass percentage of constituent as a percent

$m_{b\text{-}tot}$ – total mass of the batch

m_{con} – mass of the constituent

$m_{con\text{-}spec}$ – mass of each constituent in the specimen

m_{spec} – total mass of the specimen

mm - millimeter

psi – pounds per square inch

s – sand

sf – silica fume

sfl – silica flour

w – water

w/cm – water to cementitious materials ratio

γ – specific gravity

ε – strain

ε_{max} – highest ultimate tensile or compressive strain

ν – Poisson's ratio

%UltS – percent of ultimate stress

2 Experimental Program

Cor-Tuf ultra-high performance concrete (UHPC) is composed of eight different volume constituents that have reported compressive strengths approaching 32,000 psi (220 MPa). An experimental program was undertaken, as documented in this report, in which 254 specimens were produced from Cor-Tuf constituents.

Testing, performed on the Mississippi State University (MSU) campus, made use of raw materials provided by ERDC. Some specimens were made and cured according to protocols used at ERDC. In addition to the ERDC protocols, variations in curing, constituent proportions, and specimen size were also performed.

Standardized test methods, such as those recommended by ASTM International, are widely used and can provide some insight into numerical modeling, but often they are not intended to provide a full description of a material's behavior. As such, this report deviated from traditional test methods in some areas, as the data contained are ultimately envisioned for use with numerical models.

Specimens were tested for several properties. Tests included compressive strength according to ASTM C39 (ASTM International 2016b), elastic modulus according to ASTM C469 (ASTM International 2014), and tensile strength according to ASTM C496 (ASTM International 2011b). Some specimens were also tested while instrumented with strain gages. Volume fractions were estimated by volumetric principles, imaging programs (ImageJ, Abaqus CAE 2014), and a computed topography (CT) scan.

2.1 Constituent material properties

Eight different constituents are used to make Cor-Tuf UHPC (Table 1). The remainder of this section summarizes properties provided within manufacturer literature relative to six of the eight constituents. Air (a) is a volumetric constituent for which no data are necessary, and tap water (w) was used as needed throughout the project where the specific gravity (γ) was taken as 1.00. In this report, cementitious material (cm) was defined as cement (c) plus silica fume (sf) on a mass basis. Also, fine aggregate (fa) was defined as silica flour (sfl) plus sand (s).

Table 1. Properties of constituent materials.

Constituent	Abbreviation	Category	γ[1]	Description
Air	a	---	0.00	Air filling voids in UHPC
Water	w	---	1.00	Taken from laboratory tap
Fibers	f	---	7.85	Dramix® 3D 55/30 BG
Admixture	am	---	1.08	ADVA® 190
Cement	c	cm	3.15	API Class H (HSR) Cement
Silica Fume	sf	cm	2.25	Elkem Microsilica ES 900-W
Silica Flour	sfl	fa	2.65	SIL-CO-SIL® 75 Ground Silica
Sand	s	fa	2.65	F-50 Whole Grain Silica

[1] γ = apparent specific gravity.

Fibers (f) that were made with low carbon or mild steel and conformed to ASTM A820 (ASTM 2016a) were taken from Bekaert. These fibers have a length (l) of 3 cm, a 0.55-mm diam (D), and an aspect ratio (l/D) of 55. The fibers have a three-dimensional (3-D) geometry, a tensile strength of approximately 1.35 N/mm^2, and an elastic modulus (E) of approximately 210 N/mm^2. The primary roles of fibers within UHPC are ductility and tensile property improvements.

The admixture (am) was obtained from W.R. Grace and conformed to ASTM C494 (ASTM 2017a) Type A and F and to ASTM C1017 Type I (ASTM 2013). The admixture is a polycarboxlate-based high-range water reducer. Use of a high-range water reducer allowed the concrete to have a lower water-to-cementitious material (w/cm) ratio and higher strengths.

Cement (c) was supplied by Lafarge (a member of LafargeHolcim) out of its Joppa, IL, facility. The product meets American Petroleum Institute (API) Class H with high sulfate resistance (HSR). Table 2 summarizes properties from February to April of 2016 mill certificates. This cement is helpful for producing high ultimate strengths.

Silica fume (sf), obtained from Elkem (a Bluestar Company), had an SiO_2 of greater than 85 percent, a ZrO_2 of less than 10 percent, and a CaO of less than 4 percent. Particle sizes were approximately 0.5 microns. Silica fume lowers concrete permeability, increases corrosion resistance, and reduces the transition zone between paste and aggregates, thus increasing bond strength.

Table 2. Cement properties from mill certificates.

Property	February 2016	March 2016	April 2016	Average
Blaine fineness[1] (m^2/kg)	311	302	311	308
SiO_2 (%)	22.0	22.0	22.3	22.1
Al_2O_3 (%)	2.7	2.7	2.6	2.7
Fe_2O_3 (%)	4.5	4.5	4.4	4.5
CaO (%)	64.6	64.6	64.7	64.6
MgO (%)	2.1	2.3	2.3	2.2
SO_3 (%)	2.8	2.8	2.8	2.8
[2]Free lime (%)[1]	0.5	0.6	0.4	0.5
C_3S (%)	63	63	62	63
C_3A (%)	0	0	0	0

[1]Blaine Fineness measured via ASTM C204, and chemical properties measured via ASTM C114.

[2]1: from X-ray diffraction (XRD)

Silica flour (sfl) was obtained from US Silica™ in Berkeley Springs, WV. This material is an inert crystalline form of silica, or ground silica sand. Approximately 99 percent of the material is finer than 75 microns, and approximately 88 percenet of the material is finer than 45 microns (No. 325 sieve). Silica flour's mineralogy is quartz with a pH of 7.0. Chemically, the materials are approximately 99.5 percent SiO_2. This material is largely inert and can increase specimen density without adversely affecting hydraulic or pozzolanic reactions.

Sand (s) was obtained from US Silica™ in Ottawa, IL. The material has rounded particles of quartz mineralogy with a pH of 7.0. Approximately 98 percent of the particles pass a 425 micron (Number 40) sieve, approximately 17 percent pass a 212 micron (No. 70) sieve, approximately 3 percent pass a 150 micron (No. 100) sieve, and all are retained on a 75 micron (No. 200) sieve. Silica sand is inert, a characteristic which allows increased specimen density without affecting hydraulic or pozzolanic reactions.

2.2 Specimen preparation and curing

The materials described in Section 2.1 were utilized to make four categories of specimens for which Cor-Tuf was a baseline: UHPC, CP, (3) M, and FRP. These specimen categories are detailed in Section 2.3. Figure 1 provides photographs of key steps in the specimen preparation

and curing process applicable to all four categories. All specimen categories were prepared in essentially the same manner except that, for example, specimens without fibers omitted appropriate steps. ERDC provided baseline proportions and batching instructions for Cor-Tuf UHPC (Table 3), which were used as a reference for all specimens produced.

Table 3. Batching quantities for 0.1 ft^3 (2,832 cm^3) of Cor-Tuf (baseline condition).

Constituent	Quantity
Water	1.03 lb (467 g)
Fibers	1.54 lb (699 g)
Admixture	35.3 mL
Cement	4.92 lb (2,232 g)
Silica Fume	1.92 lb (871 g)
Silica Flour	1.36 lb (617 g)
Sand	4.77 lb (2,164 g)

Dry materials (cement, silica fume, silica flour, and sand) were weighed individually by using a digital scale then placed together into a plastic bucket and lid. Fibers were batched separately into a bowl, and admixture was poured into a graduated cylinder. Water was batched into two containers, one containing 80 percent of the water needed and another containing 20 percent of the water needed.

Once all materials were batched, the cement, silica fume, silica flour, sand, and 80 percent of the water required were poured into a tabletop mixer with paddle attachment set to a low speed (Figure 1a). Most specimens were mixed in a Hobart HL200, whereas a few specimens were mixed in a Hobart N50 5-quart mixer. Once cement, silica fume, silica flour, and 80 percent of the water were blended together, the admixture was added with the remaining 20 percent of water, which is used to rinse the graduated cylinder to ensure all admixture is incorporated (Figure 1b). These materials were then mixed for 10-15 min or until the mixture was “broken over” (reached a fluid self-consolidating consistency). The mixing bowl edges were periodically scraped (before and after mixture breaking) to ensure complete mixing. Once the mix reached a good fluidity, fibers were slowly added. Once fibers were well dispersed, mixing was completed. A total mixing time of about 20 min was typical (Figure 1c).

Figure 1. (a) Mixing dry materials and water, (b) adding admixture, (c) finished mixture, (d) vibration table, (e) specimens in curing room, (f) specimens in water bath, (g) end grinding, and (h) shelved specimens awaiting testing.

The mixture was then placed into plastic cylinder molds (2- by 4-, 3- by 6-, or 4-in. diam by 8-in. height) in two approximately equal lifts. A lift was placed, tapped around the perimeter to consolidate the mixture and remove entrapped air, and then vibrated. A vibrating table was used due to the presence of fibers, as rodding can affect fiber alignment and distribution. Vibration occurred for 1 to 2 min to remove the remaining air after tapping (Figure 1d). Once produced, specimens were stored in plastic molds with surfaces covered on a lab bench at ambient temperature for 24 to 30 hr prior to removal from molds via air pressure.

After mold removal, curing was performed with two methods: (1) a 100 percent humidity room nominally maintained at 70 to 77 °F (21° C to 25°C) (Figure 1e) and (2) water baths nominally maintained at 80 or 90 °C (Figure 1f). Water bath curing was used to replicate steam curing (i.e., placing specimens under a steam blanket and using a steam generator), as past experience at ERDC has shown submersion in 90°C water reasonably represents steam curing. Hydrated lime was not used during curing. Specimens were exposed to one of the four curing protocols, listed in the following paragraphs, prior to testing.

- Curing protocol 1 (791 °C-d): After being removed from the molds, specimens were placed in the curing room for six days (144 hr). Thereafter, specimens were placed in a water bath for 7 days (168 hr). Timing began when the specimens were placed in the bath, as it took only around 2 hr for the water to heat to the nominal temperature. The water bath started at room temperature and was then heated to a nominal 90°C to avoid thermal shock. At the conclusion of water bath curing, the bath was turned off, and the specimens were allowed to cool to ambient temperature while in the water. Once the water was at room temperature, the specimens were shelved to dry. A total of just over 14 days is required for this protocol. This protocol is usually referred to hereafter as 791 °C-days or 791 °C-d. A fairly approximate application of the ASTM C 1074 (ASTM International 2011a) maturity concept was used to calculate the °C-days for all curing protocols. The nominal laboratory bench and 100 percent humidity curing room temperature were taken as 23 °C, and the water bath temperature was taken as 90 °C (both approximate, but reasonable). As such, 23 °C * 7 days plus 90 °C * 7 days is 791 °C-d.
- Curing protocol 2 (721 °C-d): After being removed from molds, specimens were placed in the curing room for 6 days (144 hr). After 6 days, the specimens were placed in a water bath for 7 days (168 hr). Timing began when the specimens were placed in the bath, as it took around 2 hr for the water to heat to the nominal temperature. The water bath started at room temperature and was then heated to a nominal 80°C to avoid thermal shock. After 7 days, the specimens were cooled back to room temperature and shelved to dry. A total of just over 14 days was required for this protocol. The amount of curing for this protocol was approximated as 23 °C * 7 days plus 80 °C * 7 days = 721 °C-d.

- Curing protocol 3 (801 °C-d): After being removed from molds, specimens were placed in the curing room for 6 days (144 hr). After 6 days, the specimens were placed in a water bath for 8 days (168 hr). Timing began when the specimens were placed in the bath, as it took only around 2 hr for the water to heat to the nominal temperature. The water bath started at room temperature and was then heated to a nominal 80°C to avoid thermal shock. After 8 days, the specimens were cooled back to room temperature and shelved to dry. A total of just over 15 days was required for this protocol. The amount of curing for this protocol was approximated as 23 °C * 7 days plus 80 °C * 8 days = 801 °C-d.
- Curing protocol 4 (2,783 °C-d): After mold removal, specimens were placed in the 100 percent humidity curing room for 120 days. After 120 days, the specimens were removed from the curing room and shelved to dry. The amount of curing for this protocol was approximated as 23 °C * 121 days = 2,783 °C-d.

After specimens were cured and air dried for several days, they were transported to ERDC to have their ends ground to meet ASTM C39 (ASTM International 2016b) standards (Figure 1g). Once ground, mass, average diameter, and average height were measured for each specimen prior to storage ahead of mechanical property testing (Figure 1h).

2.3 Mixtures tested

Ten mixtures were produced and tested as described in Table 4. One of these mixtures was Cor-Tuf UHPC (mixture 1), while the remaining nine mixtures were subcategories of CP, M, and FRP with varying proportions. Table 4 shows the constituents and batch quantities that make up each mixture produced. In CP, M, and FRP, the constituents and batch quantities were selected to produce 0.1 ft^3 batches while maintaining desired w/cm, fa/cm, and/or f/cm ratios.

UHPC (mixture 1) was used largely as a control and frame of reference for the other categories (CP, M, and FRP). Two types of UHPC specimens were evaluated herein. The first was laboratory molded, as described in Section 2.2, and is referred to hereafter as UHPC-Base or simply as UHPC. The second type of UHPC specimen came from cores taken from a tub cast at ERDC during the work of Scott et al. (2015). Figure 2 shows the process of coring 12 specimens from this tub, nine of which were 3- by 6-in. specimens and three of which were 4- by 8-in. specimens. The average

density of these specimens was 2.52 g/cm^3 and ranged from 2.51 g/cm^3 to 2.54 g/cm^3. Three of the 3- by 6-in. cores were tested for compressive strength (elastic modulus was measured in two cases), while the remaining 9 specimens were tested for tensile strength. These cores were not cured beyond what they had already experienced upon arrival at MSU and what would occur in laboratory temperature and humidity conditions. The exact curing history of the tub was unknown.

Table 4. Batch proportions and identifiers for mixtures tested.

		Proportioning ratios			Batching quantities for 0.1 ft^3 (2,832 cm^3)						
Mixture	Identifier	w/cm	fa/cm	f/cm	Water (g)	Fibers (g)	Admixture (ml)	Cement (g)	Silica fume (g)	Silica flour (g)	Sand (g)
1	UHPC-base	0.15	0.71	0.23	467	699	35	2,232	871	617	2,164
1	UHPC-core	0.15	0.71	0.23	---	---	---	---	---	---	---
2	CP-0.11	0.11	0.00	0.00	701	---	71	4,463	1,742	---	---
3	CP-0.15	0.15	0.00	0.00	934	---	71	4,463	1,742	---	---
4	CP-0.26	0.26	0.00	0.00	1,168	---	71	4,463	1,742	---	---
5	M-0.47	0.15	0.47	0.00	619	---	47	2,957	1,154	817	1,125
6	M-0.56	0.15	0.56	0.00	619	---	47	2,957	1,154	817	1,500
7	M-0.65	0.15	0.65	0.00	619	---	47	2,957	1,154	817	1,875
8	FRP-0.11	0.15	0.00	0.11	771	577	58	3,682	1,437	---	---
9	FRP-0.17	0.15	0.00	0.17	771	864	58	3,682	1,437	---	---
10	FRP-0.23	0.15	0.00	0.23	771	1,153	58	3,682	1,437	---	---

-Water (w) was the batched amount.
--Note: all specimens were lab molded except for UHPC-Core.
--Note: batching data were not documented for UHPC-Core, but were assumed comparable to UHPC-base.

Figure 2. UHPC tub provided by ERDC (a) before, (b) during, and (c) after coring.

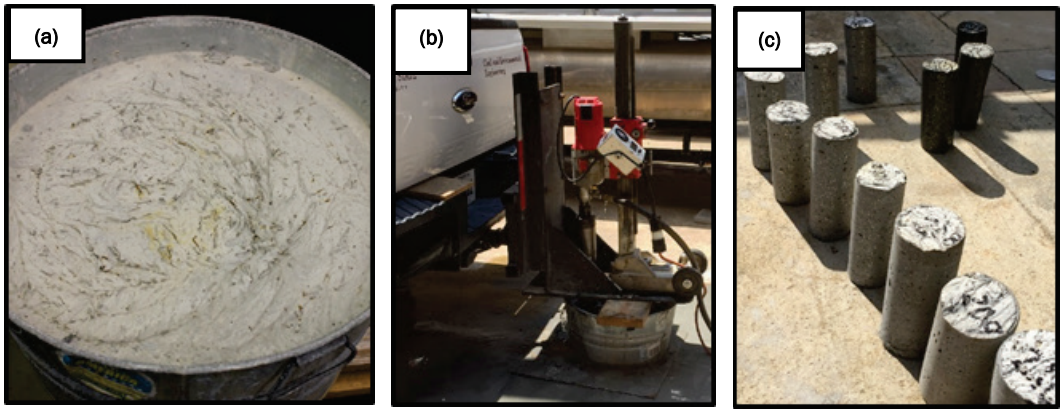

The rationale behind mixtures 2 to 10 was to vary constituent materials among categories (CP, M, and FRP) and then to vary relative proportions of constituent materials within categories (e.g., vary w/cm for CP or f/cm

for FRP). Having a suite of test results where constituents and relative proportions were varied with subsequent exposure to varied curing conditions provides a pool of mechanical properties that can be used for multi-scale modeling purposes in subsequent efforts. For CP, the water-to-cementitious material (w/cm) ratio bracketed UHPC. For M, the fine aggregate to cementitious material (fa/cm) ratio was progressively lowered below that of UHPC. For FRP, the fiber-to-cementitious material (f/cm) ratio began at the UHPC level and was progressively lowered.

2.4 Mechanical property test methods

Mechanical property testing measured compressive strength (fc), tensile strength (St), elastic modulus (E), Poisson's ratio (υ), and load (P) versus strain (ε) relationships for instrumented specimens. Mechanical property testing was performed with a Forney compression machine having a 600-kip capacity at the Construction Materials Research Center (CMRC) at Mississippi State University (MSU).

2.4.1 Compressive strength testing (non-instrumented)

Compressive strength was measured according to ASTM C39 (ASTM International 2016b) as shown in Figure 3. Specimens with ground ends were placed directly into the compression machine absent pad caps, (i.e., the concrete was directly in contact with metal on both surfaces). The load at failure was divided by the original cross-sectional area to determine the compressive strength (fc). Testing time ranged from approximately 10 to 30 min, depending on specimen strength. ASTM C39's allowable load rate is 28 to 42 psi/sec, which for the tested 3-in.-diam specimens equates to a load rate of 12 to 17.5 kips/min. As shown in Figure 3, this load rate was successfully verified.

Figure 3. Representative compressive strength test.

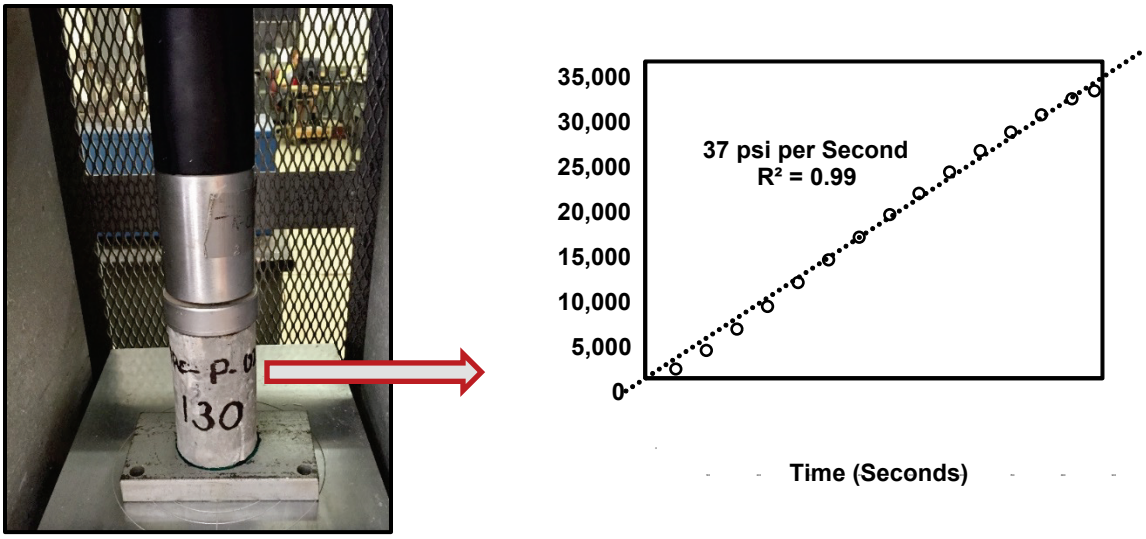

2.4.2 Elastic modulus testing (non-instrumented)

Elastic modulus was found for specimens with ends ground according to ASTM C469 (ASTM International 2014). Specimens were placed into the compression machine fitted with a compressometer (Figure 4). The compressometer recorded specimen elastic deformation with respect to applied load. By using Equation 1, the recorded deformation was able to be converted to strain.

$$\varepsilon = \frac{(d_{dial})(0.0001)}{8} \quad (1)$$

where

ε = strain experienced by the specimen
d_{dial} = displacement as taken from the dial during testing

The load was then divided by the original cross-sectional area of the specimen to obtain stress. Elastic modulus was taken as the slope of the linear portion of the stress-strain curve and is denoted E_{469} herein to associate this measurement with ASTM C469 (ASTM International 2014) and differentiate this value from elastic modulus (E) measured from other methods. Elastic modulus testing via C469 took about 45 min per specimen to complete.

Figure 4. Representative elastic modulus testing.

2.4.3 Tensile strength testing (non-instrumented)

Tensile strength was measured on specimens according to ASTM C496 (ASTM International 2011b; Figure 5). The specimens were placed on their sides and had two bearing strips (1/8-in.-thick plywood) placed between the machine and the specimen (i.e., there was always a barrier of wood between the specimen and the metal surfaces on the top and bottom). These thin pieces of wood helped distribute the applied load uniformly throughout the specimen. The maximum applied load was recorded and used to find tensile strength by using Equation 2. Since the load rate for this test was 3.3 psi/sec or less, experiments ranged from approximately 30 to 120 min, depending on the specimen.

$$\mathrm{St} = \frac{2P}{\pi l D} \tag{2}$$

where

St = splitting tensile strength (MPa)
P = maximum applied load (N)
l = length of the specimen (mm)
D = diameter of the specimen (mm)

Figure 5. Representative tensile testing.

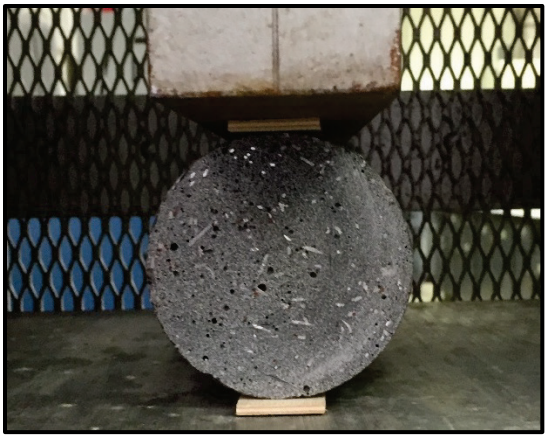

2.4.4 Compressive and tensile testing instrumented with strain gages

Foil strain gages (SG) are a versatile method for measuring responses that can be used for numerical modeling purposes. Example applications range from strain measurement on materials much less stiff than concrete, such as geogrids and geotextiles (Warren et al. 2010), to materials besides concrete with stiffnesses on the order of concrete, such as fiber reinforced polymers (Howard and GangaRao 2009), to materials stiffer than concrete, such as metal (Rushing et al. 2016).

Vishay Micro-Measurements 350 Ω general purpose gages (C2A-06-125-Lw-350 and C2A-06-250LW-350) were attached to specimens using M-Bond 200 glue and catalyst following instructions given by Vishay. The strain gages were then connected to a National Instruments NI CompaqDaq 9172 chassis and NI 9237 I/O modules that recorded all of the data collected from the gages at a rate of slightly less than 5 Hz by using a program written in LabVIEW. Instrumented specimens were tested in compression, and additional instrumented specimens were tested in tension (Figure 6). Appendix A provides drawings of strain gage locations, where strain gages are denoted SG-0 through SG-3. Elastic modulus was also found locally by using strain gages and is reported in Section 3.4 as E_{SG-0} through E_{SG-3}.

Figure 6. (a) Compressive testing, (b) elastic modulus testing, and (c) tension testing with strain gages.

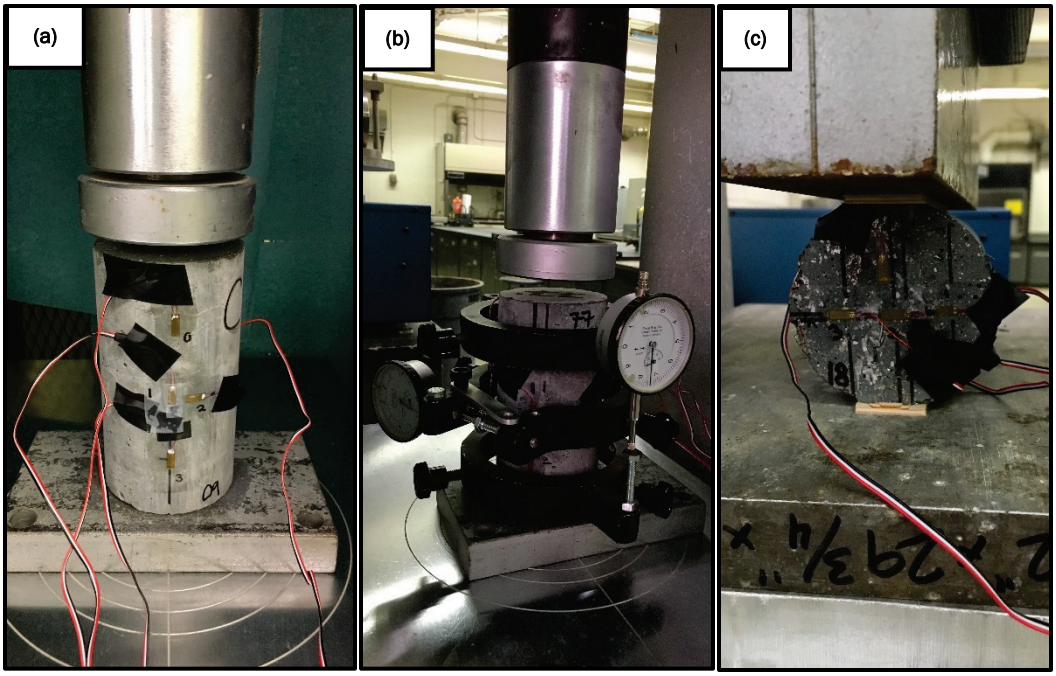

2.5 Volume fractions

2.5.1 As-batched volume estimations

Volume fractions were estimated by way of batch quantities and constituent material specific gravity values. To find these volumetric estimations, two critical assumptions were necessary. The first assumption was that the aggregates used do not absorb water. This is reasonable considering the fine aggregates used have less than 0.25 percent water absorption, based on past tests conducted by ERDC on these materials. The second assumption was that the amount of water batched remained constant until the specimen was tested. It is important to note that the volume fractions calculated from as-produced densities and as-batched quantities are estimates and do not account for volume change during hydration, nor do they provide any information on distribution and size of air voids. All of the batching masses for each constituent were recorded as well as the final weight of each specimen. From the batching masses, the mass percentage of the constituents was found for each specimen by using Equation 3.

$$m_{b-per} = \frac{m_{con}}{m_{b-tot}} \tag{3}$$

where

m_{con} = mass of the constituent in grams
$m_{b\text{-}tot}$ = total mass of the batch in grams
$m_{b\text{-}per}$ = batching mass percentage of constituent as a percent

This percentage was multiplied by the weight of each specimen to get the ideal weight of each constituent in each specimen shown in Equation 4.

$$m_{con-spec} = (m_{b-per})(m_{spec}) \quad (4)$$

where

$m_{b\text{-}per}$ = batching mass percentage of constituent as a percent
m_{spec} = total mass of the specimen in grams
$m_{con\text{-}spec}$ = mass of each constituent in the specimen in grams

These masses were then divided by their specific gravity and then summed to find a specimen volume with no air, shown in Equation 5.

$$V_{noair} = \sum \frac{m_{con-spec}}{\gamma} \quad (5)$$

where

$m_{con\text{-}spec}$ = mass of each constituent in the specimen in grams
γ = specific gravity of the constituent
V_{noair} = volume of the specimen if there was no air in g/cm^3

The volume of air (V_a) was then found by finding the difference between the laboratory recorded volume of the specimen (found by taking average heights, diameters, and masses) and the ideal volume of the specimen with no air (V_{noair}). V_{noair} is the sum of cement volume (V_c), silica fume volume (V_{sf}), silica flour volume (V_{sfl}), sand volume (V_s), water volume (V_w), fibers volume (V_f), and admixture volume (V_{am}). Each of these volumes was determined with its corresponding $m_{con\text{-}spec}$ and specific gravity.

2.5.2 Volume fractions from imaging techniques

Some specimens were used for an imaging analysis to estimate volume fractions. These volume fractions were found by taking pictures of the specimens then using the programs ImageJ and Abaqus to find volume fractions. Lower magnification images were taken using a ZEISS Axiovert 200 optical microscope at the Center for Advanced Vehicular Systems

(CAVS) at Mississippi State University. A scanning electron microscope model SUPRA 40 FEG-SEM, also at CAVS, was used to take higher magnification images. The surfaces of the specimens were ground smooth before imaging to ensure quality pictures. The combination of the low and high magnification microscopes allowed for images to be taken at varying length scales to capture the size distributions of each constituent.

The image processing tool, ImageJ, was used for analyzing images (Schneider et al. 2012). This software was utilized to identify, isolate, and measure constituents (Figure 7). These results allowed for the determination of the average size, number density, area fraction, and nearest neighbor distance of each constituent. ImageJ was used on multiple images at varying length scales to ensure accurate results were found for each of the constituents.

Figure 7. ImageJ process for turning (a) scanning electron microscope images to a (b) binary image and then (c) isolating inclusions

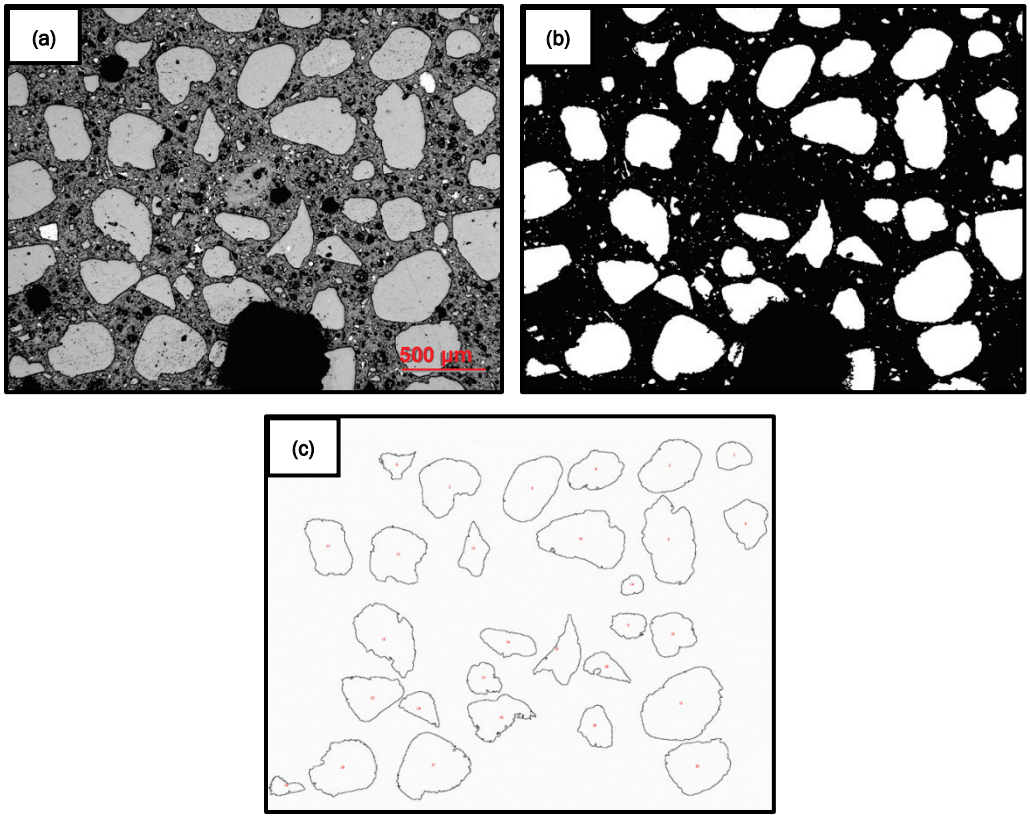

The finite element software Abaqus was used to generate representative volume element (RVE) cubes to portray UHPC (Abaqus 2014). It was determined that three length scales would aid modeling of UHPC mesoscale characteristics, as there were such differences in the size of

constituents. The largest cube had sides of 35 mm, and it included only steel fibers within the matrix. The middle length scale included large voids and silica sand grains and had sides of 0.54 mm. The smallest length scale was a cube with sides of 0.04 mm, and it included small voids and unhydrated cement grains.

To best portray the material, inclusions were randomly distributed throughout the matrix according to their measured distributions. Results from ImageJ gave an area fraction, while Abaqus required a volume fraction for geometry generation. The average size of each inclusion type was assumed to be the area of a circle, and the average radius was found. For the geometry generation, the area fraction was assumed to be the same as the volume fraction, and the average radius size was used to create spheres and cylinders.

A python script was written to generate these RVE cubes. This script required inputs for average inclusion size (found using ImageJ), and inclusions of that size were inserted into the matrix until the desired volume fraction was reached. Plots of constituent size versus number of occurrences revealed that using only the average constituent size left out the range of inclusion sizes found in UHPC. The size versus number of occurrences graph was fitted with a distribution curve, and a second script was created that required the mean and variance of this fitted curve. The inclusions inserted into the matrix by this second code were of sizes that varied according to the distribution curve.

Both random generation codes required the size of the cube, as well as the number, shape, and volume fraction of each constituent. Two shapes, spheres and cylinders, were used in modeling the inclusions in subsequent simulations. Spheres were used to model the voids, unhydrated cement grains, and sand grains; cylinders were used to model the steel fibers. The algorithms then randomly inserted and distributed these shapes, making sure none overlapped. Figure 8 represents the RVE generations.

Figure 8. Geometries generated using the area fractions and length scales found through image analysis.

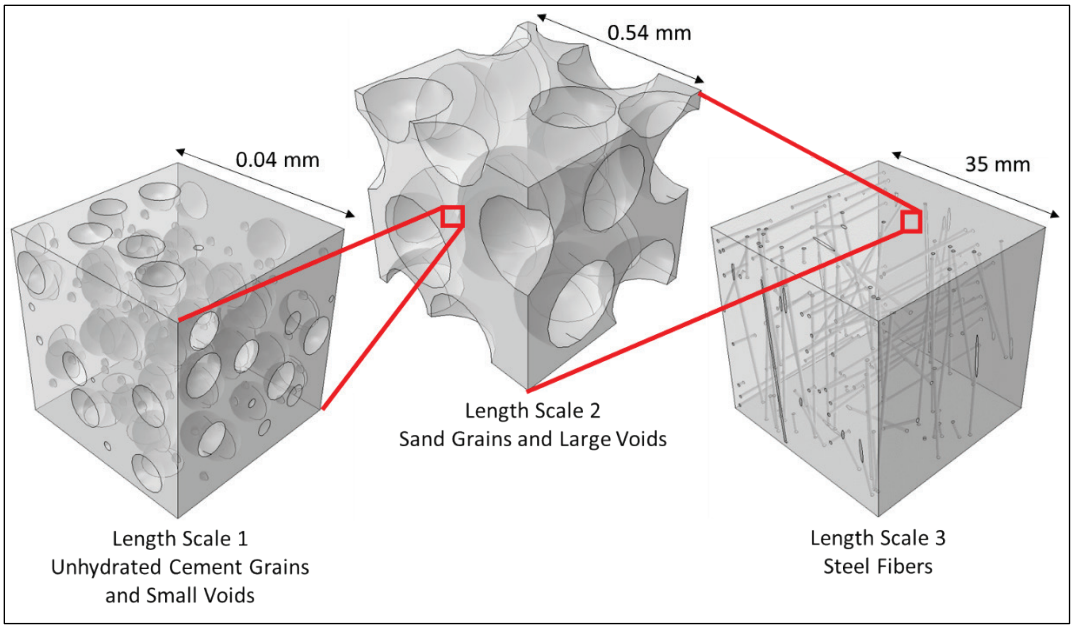

The Phoenix X-Ray Computed Topography (CT) system with dual focus, reaching one-micron resolution, located at CAVS, was used for 3-D imaging. CT scans were conducted on a UHPC cube with sides of approximately 50 mm. The CT scan distinguished the larger constituents, large voids, and steel fibers, helping to determine the 3-D characteristics of UHPC.

2.6 Test matrix

Table 5 is the test matrix for the 254 specimens produced and tested for this report. This matrix evaluated specimens of the four consistent categories (UHPC, CP, M, and FRP) at different specimen sizes (2 by 4 to 4 by 8) and after different amounts of curing (721 to 2,783 °C-d) for mechanical properties and/or volume fractions. Eight of the mechanical property specimens were instrumented with strain gages, and several of the compression specimens were fitted with a compressometer for elastic modulus determination. Volume fractions were measured by imaging on the five specimens shown in Table 5 and were also estimated on the mechanical property specimens by way of mass proportions and specific gravities.

Table 5. Testing matrix

			Mechanical property specimens		Volume fractions
Mix	Curing	Size	Compression	Tension	Imaging
UHPC	2,783 °C-d	3x6	6	6	0
CP-0.15[1]	2,783 °C-d	3x6	15	3	0
CP-0.15[1]	2,783 °C-d	2x4	9	0	0
M-0.56	2,783 °C-d	3x6	6	3	0
FRP-0.23[2]	2,783 °C-d	3x6	10	11	0
FRP-0.23[2]	2,783 °C-d	4x8	2	3	0
UHPC	791 °C-d	3x6	6	3	2
CP-0.15	791 °C-d	3x6	6	3	1
CP-0.11	791 °C-d	3x6	6	3	0
CP-0.26	791 °C-d	3x6	6	3	0
M-0.56	791 °C-d	3x6	6	3	1
M-0.47	791 °C-d	3x6	6	3	0
M-0.65	791 °C-d	3x6	6	3	0
FRP-0.23	791 °C-d	3x6	6	3	1
FRP-0.17	791 °C-d	3x6	6	3	0
FRP-0.11	791 °C-d	3x6	6	3	0
UHPC	721 °C-d	3x6	6	3	0
CP-0.15	721 °C-d	3x6	6	3	0
M-0.56	721 °C-d	3x6	6	3	0
FRP-0.23	721 °C-d	3x6	6	3	0
UHPC[3]	801 °C-d	3x6	6	3	0
CP-0.15	801 °C-d	3x6	6	3	0
M-0.56	801 °C-d	3x6	6	3	0
FRP-0.23	801 °C-d	3x6	6	3	0
UHPC-Core	Core	3x6	3	6	0
UHPC-Core	Core	4x8	0	3	0
All Specimens			159	89	5

[1]: 2x4 and 3x6 specimens were sometimes produced in the same batch for paired comparisons.

[2]: 3x6 and 4x8 specimens were sometimes produced in the same batch for paired comparisons.

[3]: One additional specimen (shown in Figure 3) was produced for protocol development, but was not included in the data reported in Chapter 3 (i.e., there were 7 compression specimens, but only 6 were included in Chapter 3).

3 Test Results

The Table 5 testing matrix was largely divided into behaviors of interest for reporting purposes. Some specimen types had multiple property measurements, and as a result, reporting the data in this manner seemed more logical.

3.1 Varying proportions

Of the 254 specimens produced, 90 were tested after 791 °C-d curing to assess the effects of varying proportions on fundamental properties; 10 different types of specimens were tested (Table 6). The densities of these specimens ranged from 2.14 g/cm³ to 2.61 g/cm³, and all were 3-in. diam by 6-in. height. Figures 9 and 10 show side-by-side comparisons of the variations data for compressive and tensile testing.

Table 6. Varying proportions test results.

Mix ID	fc Range (MPa)	fc COV (%)	fc Avg. (MPa)	St Range (MPa)	St COV (%)	St Avg. (MPa)	Density Range (g/cm³)	Density COV (%)	Density Avg. (g/cm³)
UHPC	152.4 – 203.1	12.0	***175***	19.5 – 26.1	14.5	***23***	2.467 – 2.608	1.6	***2.52***
CP-0.11	68.1 – 141.0	26.4	***117***	8.1 – 10.4	13.6	***10***	2.224 – 2.286	0.9	***2.27***
CP-0.15	77.7 – 167.7	24.6	***117***	9.7 – 12.8	14.3	***12***	2.230 – 2.275	0.7	***2.25***
CP-0.26	81.5 – 137.8	19.0	***113***	3.7 – 8.9	40.1	***7***	2.140 – 2.183	0.7	***2.17***
M-0.47	139.8 – 175.4	7.6	***161***	7.7 – 13.7	29.8	***12***	2.247 – 2.297	0.8	***2.26***
M-0.56	122.2 – 155.1	9.1	***141***	9.3 – 12.9	17.3	***12***	2.233 – 2.314	1.1	***2.27***
M-0.65	146.0 – 192.5	11.2	***164***	9.4 – 15.3	27.0	***12***	2.254 – 2.292	0.6	***2.27***
FRP-0.11	93.6 – 132.0	12.5	***116***	19.1 – 25.1	13.7	***22***	2.347 – 2.412	1.0	***2.39***
FRP-0.17	109.3 – 139.9	9.3	***125***	13.9 – 26.0	30.2	***21***	2.436 – 2.515	1.1	***2.47***
FRP-0.23	120.7 – 141.9	6.4	***135***	26.3 – 26.6	0.5	***26***	2.465 – 2.584	1.6	***2.51***

–Note: Averages include 6 fc, 3 St, and 9 densities.

UHPC had the highest compressive strength, followed by M, FRP, and CP. CP was not sensitive to w/cm ratio changes within the range considered, M did not respond in a progressive manner as the fa/cm ratio was changed, and FRP increased compressive strength as the f/cm ratio increased. Several of the results from varying proportions were not intuitive.

FRP with the highest fiber loading produced the highest tensile strength. Overall, UHPC and FRP had comparable tensile strengths. M tensile strength was insensitive to fa/cm ratio changes. CP behaved somewhat erratically in tension and produced the lowest overall strength. Overall, tensile strength behaviors were fairly intuitive.

Figure 9. Average compressive strength for 791 °C-d cured specimens.

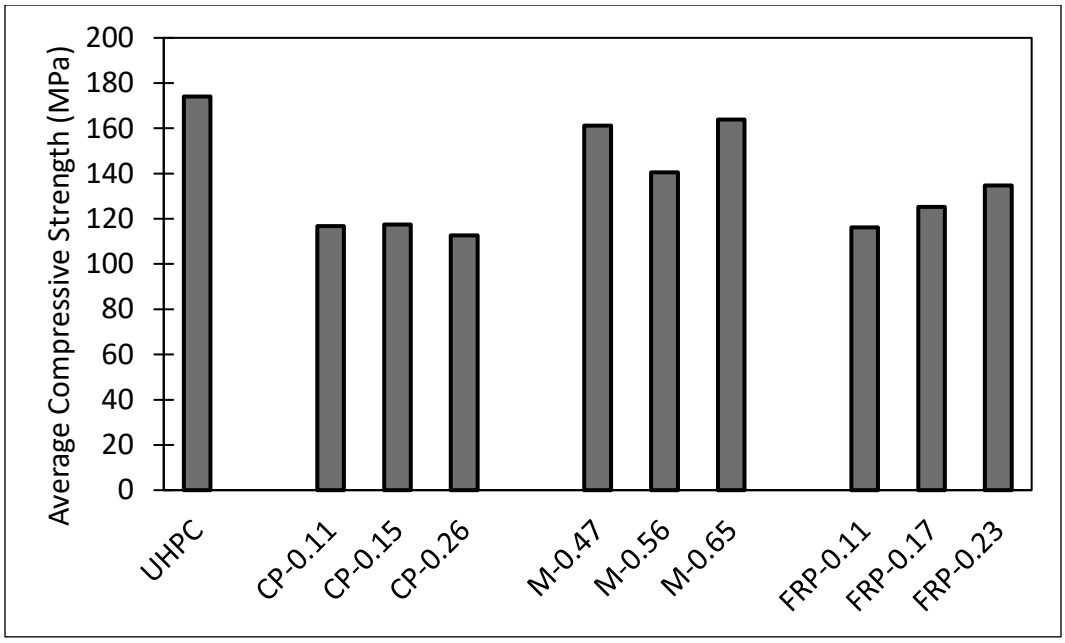

Figure 10. Average tensile strength for 791 °C-d cured specimens.

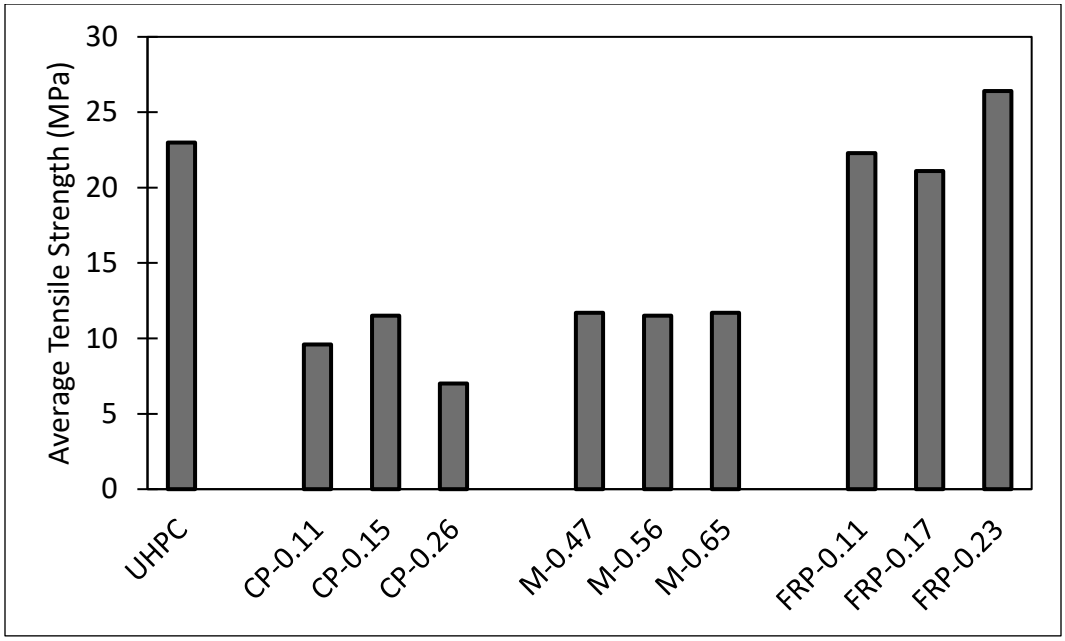

Elastic modulus was also found for specimens that underwent compressive testing in accordance to ASTM C469 (ASTM International 2014). The relationship between elastic modulus and compressive strength is often reported in the form of Equation 6. The constant relating elastic modulus and compressive strength is the parameter of primary interest, and Table 7 reports all C_{469} findings.

$$E_{469} = C_{469}\sqrt{f_c} \quad (6)$$

where

E_{469} = elastic modulus from ASTM C469 (MPa; ASTM International 2014))
C_{469} = constant
f_c = compressive strength (MPa)

Table 7. Elastic modulus and ultimate strength constant for varying proportions.

Mix ID	Curing	E_{469} Range (MPa)	Avg. E_{469} (MPa)	COV (%)	C_{469} Range	COV (%)	C_{469} Avg.
UHPC	791 °C-d	49,509 – 49,617	***49,600***	0.1	3,848 – 4,013	3.0	***3,931***
CP-0.15	791 °C-d	33,826 – 36,682	***35,300***	5.7	3,235 – 3,433	4.2	***3,334***
M-0.56	791 °C-d	41,547 – 45,296	***43,400***	6.1	3,489 – 3,637	2.9	***3,563***
FRP-0.23	791 °C-d	31,460 – 32,374	***31,900***	2.0	2,776 – 2,947	4.2	***2,862***
CP-0.11	791 °C-d	40,884 – 41,786	***41,300***	1.5	3,443 – 3,654	4.2	***3,548***
CP-0.26	791 °C-d	27,887 – 28,355	***28,100***	1.2	2,576 – 3,142	14.0	***2,859***
M-0.47	791 °C-d	43,830– 45,564	***44,700***	2.7	3,371 – 3,637	5.4	***3,504***
M-0.65	791 °C-d	45,104 – 45,764	***45,434***	1.0	3,564 – 3,726	3.1	***3,645***
FRP-0.17	791 °C-d	32,116 – 38,420	***35,300***	12.6	2,873 – 3,674	17.3	***3,273***
FRP-0.11	791 °C-d	30,278 – 34,821	***32,500***	9.9	2,811 – 3,600	17.4	***3,206***

–Note: Above averages include 2 E_{469} values and 2 C_{469} values.

The American Concrete Institute (ACI) document 318 allows the constant relating elastic modulus to compressive strength in the form of Equation 6 to be 57,000 for U.S. customary units (i.e., psi). For SI units (i.e., MPa), this constant is approximately 4,700. The main observation from Table 7 is that the materials evaluated do not produce as high of an elastic modulus per unit of compressive strength as typical ready-mixed concrete.

3.2 Curing effects

Of the 254 specimens produced, 153 were utilized to assess curing effects on mechanical properties. Most of the data were from laboratory molded specimens, with a small assessment from nine cores. Laboratory molded data were reported first, followed by a brief assessment with the core test results.

3.2.1 Curing effects measured on laboratory molded specimens

Of the 254 specimens produced, 144 were utilized to assess curing effects on mechanical properties from laboratory molded specimens (Table 8). Note that 791 °C-d data are replicated between Table 6 and Table 8. Table 8 utilized six compression and three tensile specimens per mix at a given type of curing. All nine of these specimens were used to assess density, which ranged from 2.19 to 2.64 g/cm^3.

Table 8. Curing effects test results.

Mix ID	Curing	fc Range (MPa)	fc COV (%)	fc Avg. (MPa)	St Range (MPa)	St COV (%)	St Avg. (MPa)	Density Range (g/cm³)	Density COV (%)	Density Avg. (g/cm³)
UHPC	791 °C-d	152.4 – 203.1	12.0	***175***	19.5 – 26.1	14.5	***23***	2.467 – 2.608	1.6	***2.52***
CP-0.15		77.7 – 167.7	24.6	***117***	9.7 – 12.8	14.3	***12***	2.230 – 2.275	0.7	***2.25***
M-0.56		122.2 – 155.1	9.1	***141***	9.3 – 12.9	17.3	***12***	2.233 – 2.314	1.1	***2.27***
FRP-0.23		120.7 – 141.9	6.4	***135***	26.3 – 26.6	0.5	***26***	2.465 – 2.584	1.6	***2.51***
UHPC	721 °C-d	156.2 – 183.6	7.1	***170***	22.1 – 28.8	15.5	***24***	2.487 – 2.554	0.8	***2.53***
CP-0.15		106.4 – 170.1	18.7	***124***	4.5 – 11.1	41.6	***9***	2.223 – 2.261	0.6	***2.24***
M-0.56		138.6 – 208.4	15.4	***179***	11.0 – 12.6	7.2	***12***	2.262 – 2.347	1.4	***2.30***
FRP-0.23		88.3 – 120.5	12.9	***105***	17.3 – 23.6	17.3	***20***	2.460 – 2.547	1.1	***2.52***
UHPC	801 °C-d	155.5 – 221.5	14.5	***190***	18.7 – 23.8	12.7	***21***	2.453 – 2.605	1.8	***2.51***
CP-0.15		108.9 – 167.5	20.9	***135***	4.0 – 10.5	44.6	***8***	2.191 – 2.265	1.1	***2.23***
M-0.56		120.4 – 187.4	18.3	***161***	10.8 – 14.0	13.0	***13***	2.255 – 2.309	0.9	***2.28***
FRP-0.23		74.9 – 145.9	20.4	***119***	22.2 – 24.9	6.0	***24***	2.479 – 2.644	2.1	***2.56***
UHPC	2,783 °C-d	131.5 – 163.4	7.5	***149***	18.8 – 22.3	8.9	***21***	2.527 – 2.577	0.7	***2.55***
CP-0.15		78.0 – 143.4	21.0	***109***	4.7 – 10.1	47.6	***7***	2.188 – 2.274	1.6	***2.24***
M-0.56		126.3 – 144.8	6.1	***136***	10.3 – 12.0	8.2	***11***	2.253 – 2.310	0.9	***2.28***
FRP-0.23		113.9 – 135.8	6.6	***122***	19.6 – 27.7	17.0	***24***	2.457 – 2.623	2.0	***2.53***

--Note: Above averages include six fc, three St, and nine densities.

As seen in Table 5, there were often more than six compression and three tension specimens tested after 2,783 °C-d curing. In these cases, the first six compression measurements and/or the first three tension measurements were utilized in Table 8 for consistency across all curing protocols. The additional replicates for 2,783 °C-d curing were performed for investigations reported later in this chapter. Figures 11 to 18 plot the results from

Table 8. Figures 11 and 12 are bar charts comparing curing effects on tensile and compressive strength. Figures 13 to 18 are equality plots comparing curing protocols 721, 801, and 2,783 °C-d to ERDC's baseline protocol of 791 °C-d, where the specimens are exposed to 90 °C water.

Figure 11. Average compressive strength of curing variations.

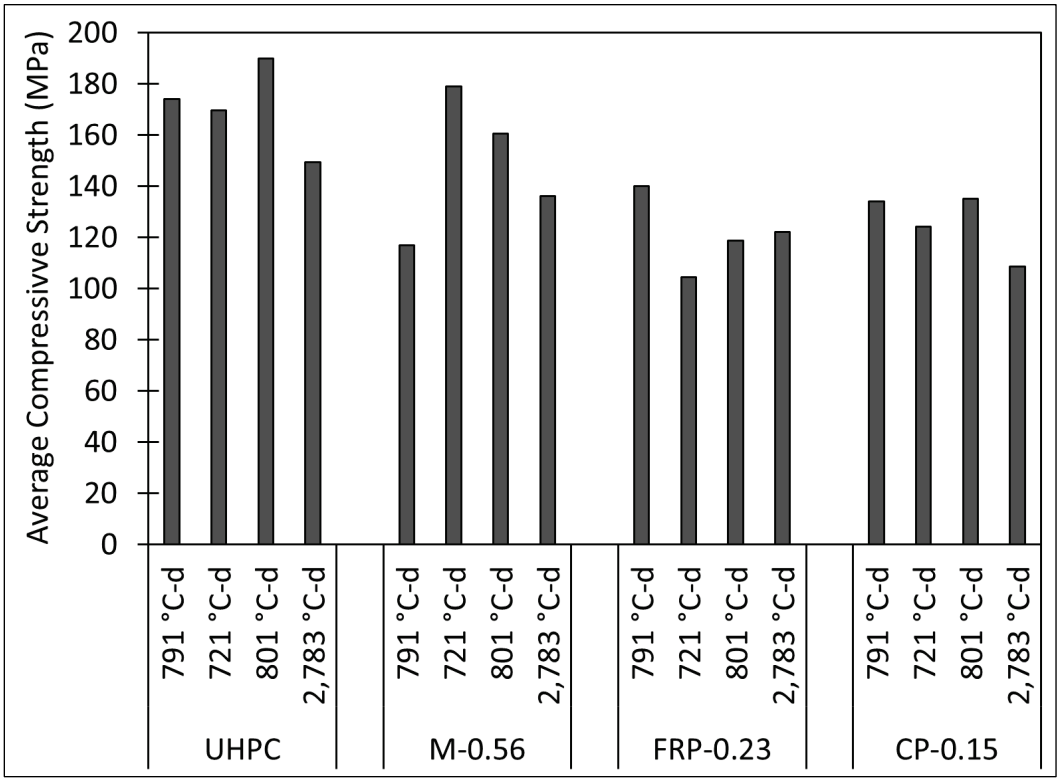

Figure 12. Average tensile strength of curing variations.

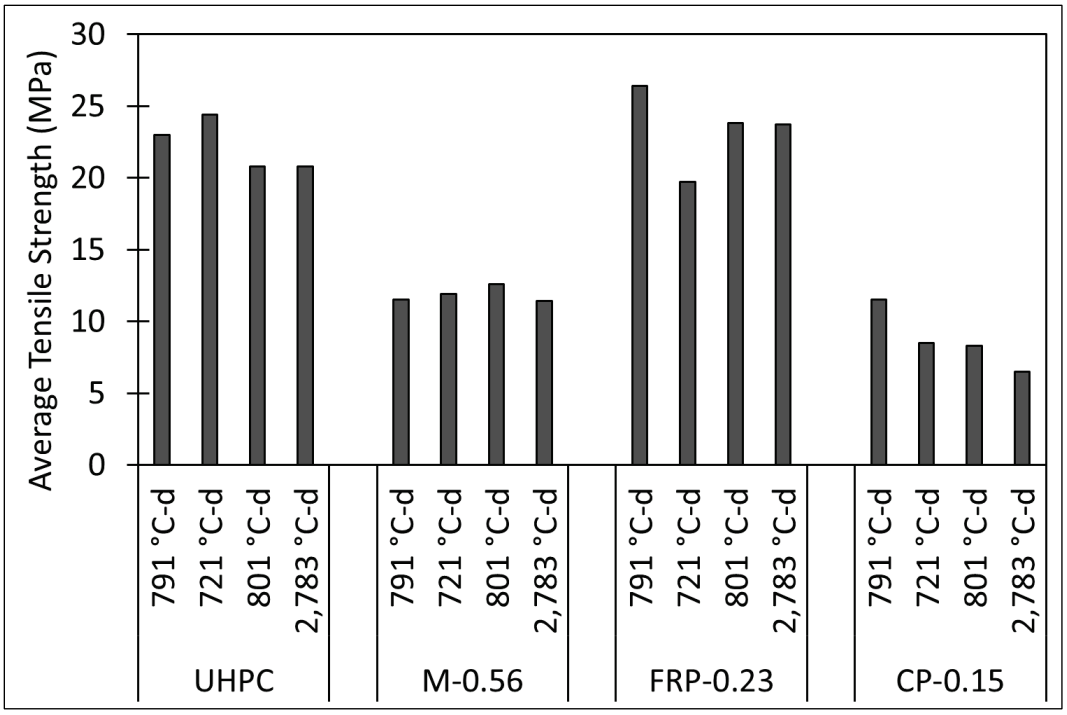

Figure 13. 721 °C-d curing versus 791°C-d curing in compression.

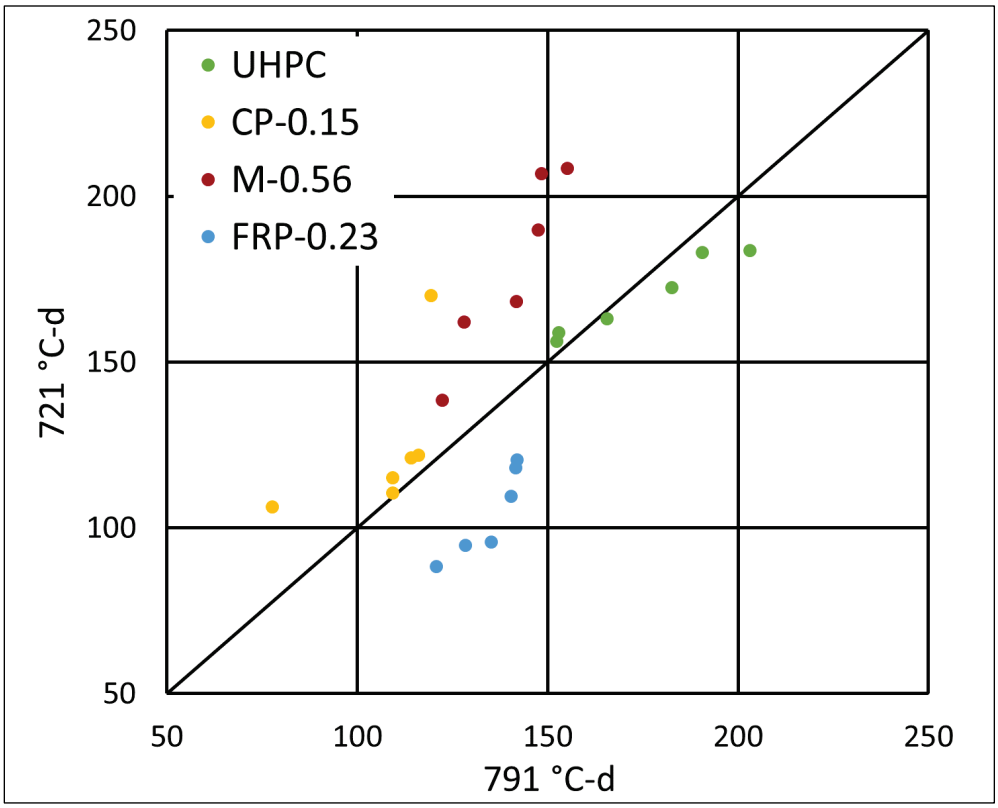

Figure 14. 801 °C-d curing versus 791 °C-d curing in compression.

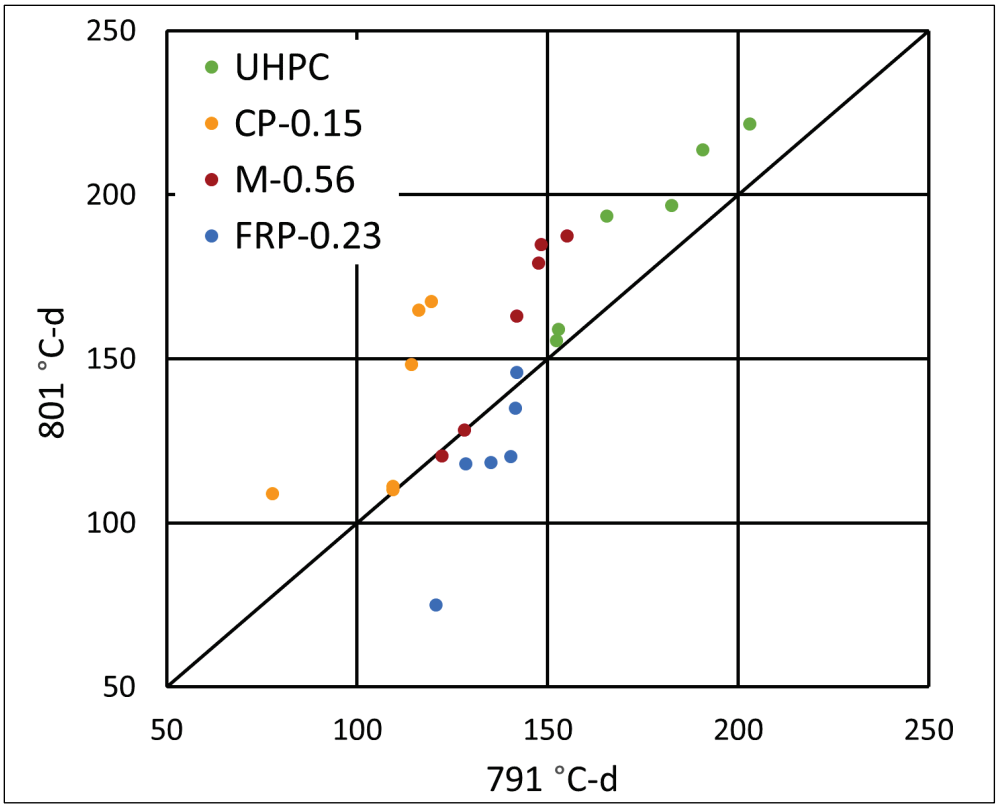

Figure 15. 2,783 °C-d curing versus 791 °C-d curing in compression.

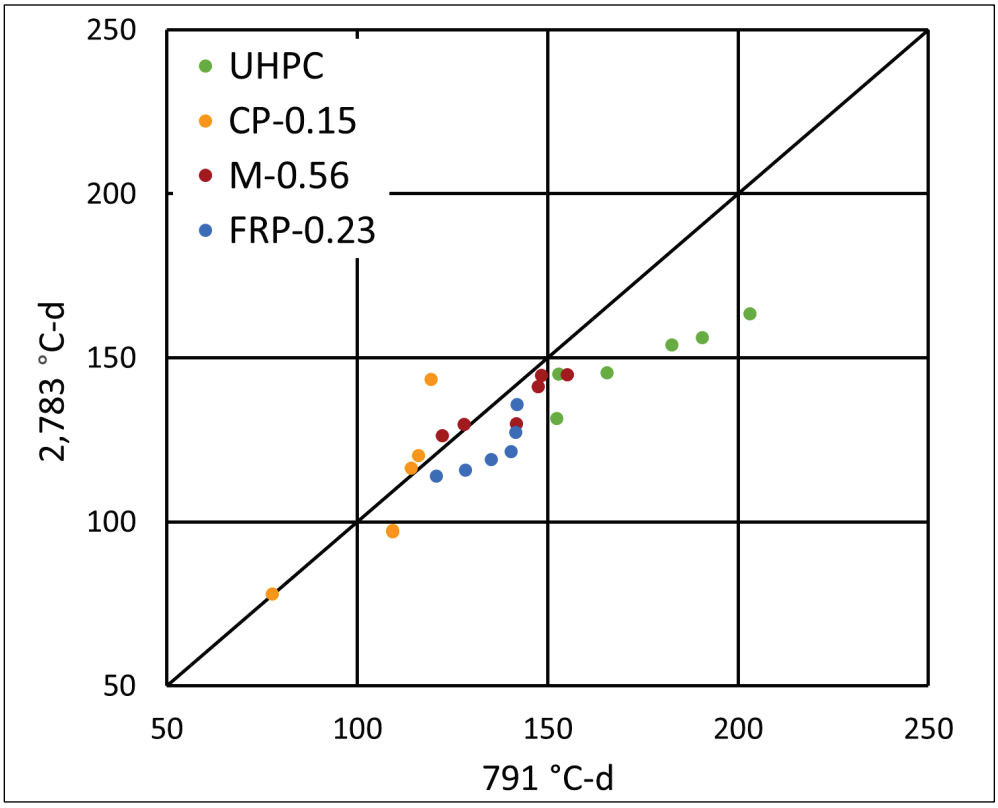

Figure 16. 721 °C-d curing versus 791 °C-d curing in tension.

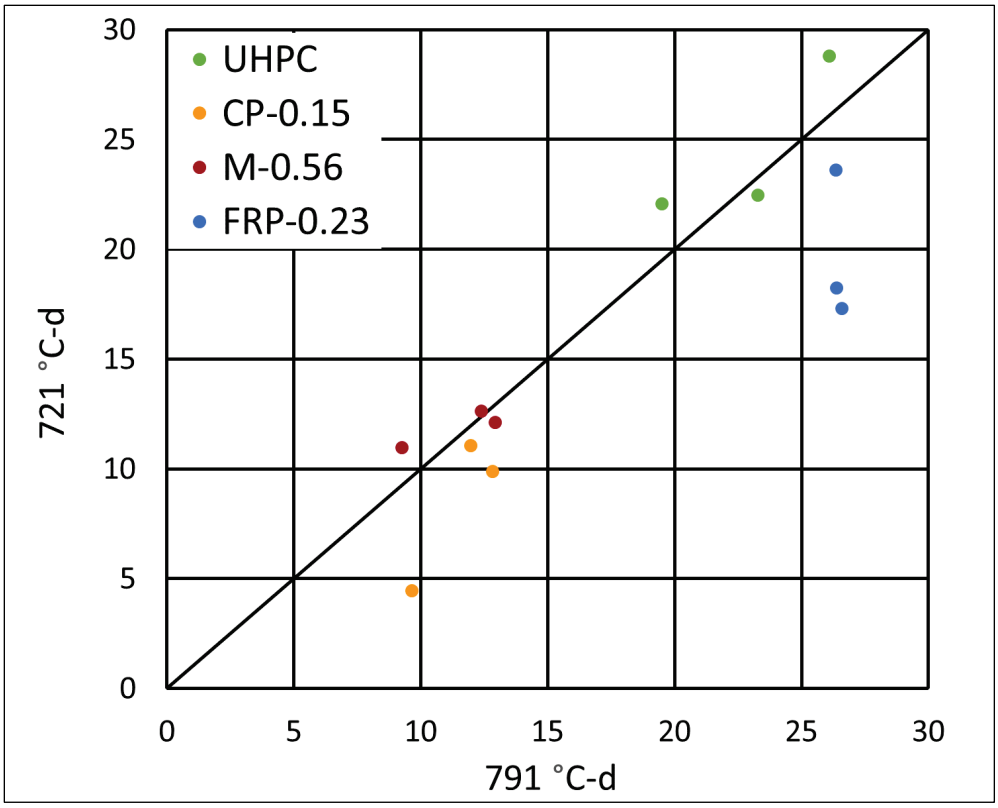

Figure 17. 801 °C-d curing versus 791 °C-d curing in tension.

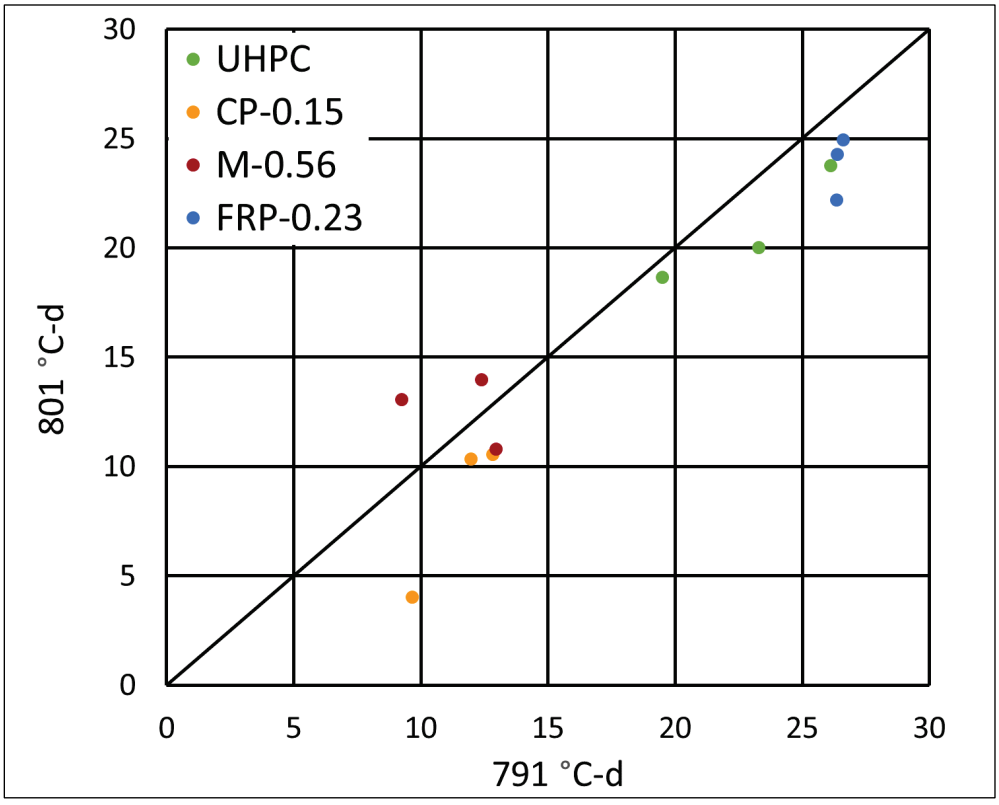

Figure 18. 2,783 °C-d curing versus 791 °C-d curing in tension.

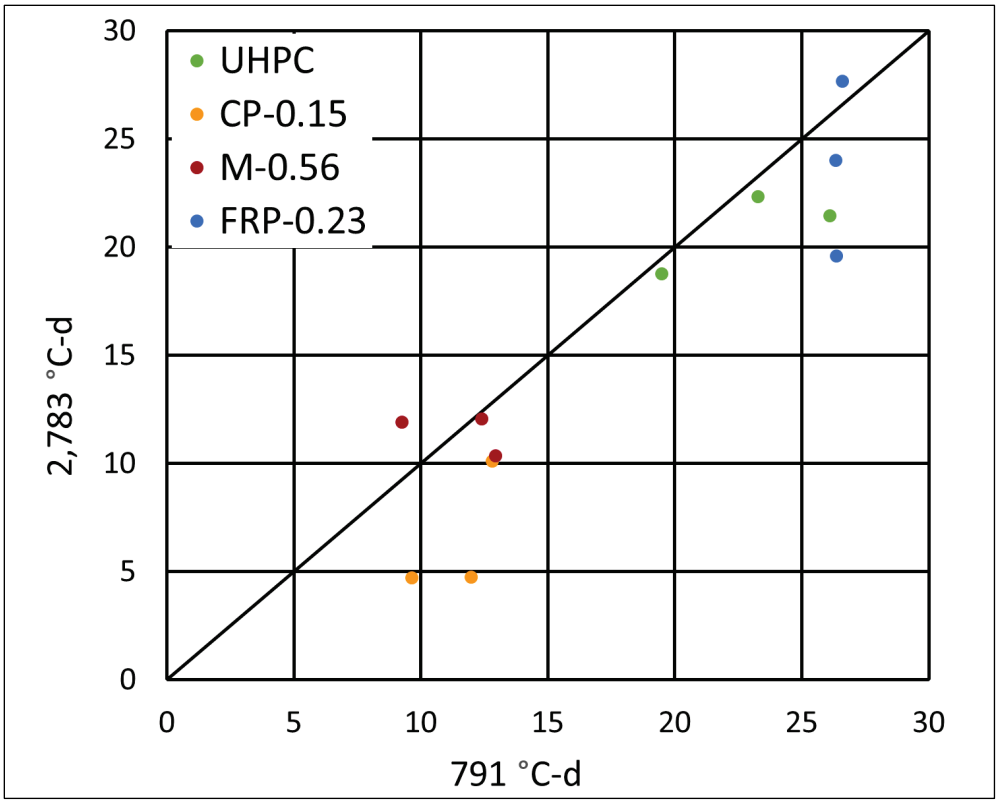

Curing protocols noticeably impacted compressive strength for all specimen types. Curing protocols noticeably affected UHPC, CP, and FRP tensile strength, but did not noticeably affect M.

Figures 13 and 14 were used to make the following assessments regarding compressive strength. UHPC seemed to respond better to 80 °C curing than 90 °C curing for a comparable level of °C-days. This same trend was observed with M and CP, but not with FRP. FRP clearly deviated from the other categories for 80 °C curing relative to 90 °C curing, as 90 °C curing produced higher strengths.

Figure 15 was used to make the following assessments about compressive strength. In compression, all UHPC and FRP specimens were stronger after 791 °C-d of curing, for which 90 °C was utilized, relative to 3.5 times the amount of °C-days (2,783), for which temperature was 23 °C. CP was comparable, where M might have slightly favored 90 °C curing for less °C-days. Overall, the data were below the equality line, indicating curing at higher temperatures for less °C-days produced higher compressive strength than lower temperatures for more °C-days.

Figures 16 and 17 were used to make the following assessments about tensile strength. UHPC's response was not definitive. The 721 °C-d specimens with 80 °C curing were modestly stronger than the 791 °C-day specimens with 90 °C curing, suggesting 80 °C curing was more favorable. The opposite behavior, however, was observed when 801 °C-d at 80 °C curing was compared to 791 °C-d at 90 °C curing. CP favored 90 °C curing, which was opposite to compressive strength testing in Figures 13 and 14. M seemed largely indifferent to curing protocol when tested in tension. FRP favored 90 °C curing, which agrees with the behavior observed in compression (Figures 13 and 14).

Figure 18 was used to make the following assessments about tensile strength. UHPC favored 90 °C curing, which matched its behavior in compression in Figure 15 (i.e., that fewer °C-days of a higher temperature produced better properties). CP also favored 90 °C curing, which disagreed with its compressive strength behavior. M seemed largely indifferent to the curing protocol. FRP generally favored 90 °C curing.

The main observation from Table 8 (and Figures 11 to 18 that plotted data from Table 8) is that the specific aspects of curing seem to affect compressive and tensile properties and that the effects are not consistent between tension and compression or between specimen category (UHPC, CP, M, or FRP). These data suggest that only accumulating °C-days and using that number as a maturity index may lead to undesirable outcomes for some types of UHPC endeavors. For large placements of UHPC where very large temperature fluctuations with space and time are expected, more understanding of how UHPC responds to time, temperature, and their interaction seems useful. This same understanding is needed to further develop multiscale models of high-strength concrete.

Curing effects on elastic modulus are shown in Table 9. The main observation is that the materials evaluated do not produce as high of an elastic modulus per unit of compressive strength as typical ready-mixed concrete.

Table 9. Elastic modulus and ultimate strength constant for varying curing.

Mix ID	Curing	E_{469} Range (MPa)	E_{469} COV (%)	E_{469} Avg. (MPa)	C_{469} Range	COV (%)	C_{469} Avg.
UHPC	791 °C-d	49,509 – 49,617	0.1	***49,600***	3,848 – 4,013	3.0	***3,931***
CP-0.15		33,826 – 36,682	5.7	***35,300***	3,235 – 3,433	4.2	***3,334***
M-0.56		41,547 – 45,296	6.1	***43,400***	3,489 – 3,637	2.9	***3,563***
FRP-0.23		31,460 – 32,374	2.0	***31,900***	2,776 – 2,947	4.2	***2,862***
UHPC	721 °C-d	51,810 – 57,633	5.3	***54,800***	4,059 – 4,611	7.5	***4,246***
CP-0.15		31,699 – 37,223	8.7	***35,200***	3,073 – 3,425	5.8	***3,293***
M-0.56		44,626 – 50,060	5.7	***47,500***	3,467 – 3,505	0.6	***3,484***
FRP-0.23		29,684 – 31,196	2.5	***30,400***	2,890 – 3,206	5.5	***3,085***
UHPC	801 °C-d	51,633 – 54,474	2.7	***52,900***	3,660 – 3,747	1.2	***3,706***
CP-0.15		35,747 – 39,371	4.9	***37,400***	3,034 – 3,390	6.2	***3,163***
M-0.56		44,095 – 47,617	4.1	***45,500***	3,221 – 3,503	4.8	***3,409***
FRP-0.23		28,268 – 31,828	5.9	***30,100***	2,579 – 2,924	6.3	***2,757***
UHPC	2,783 °C-d	48,269 – 50,001	1.9	***49,000***	3,922 – 4,209	3.7	***4,044***
CP-0.15		31,284 – 31,715	0.7	***31,500***	2,638 – 3,542	15.4	***3,024***
M-0.56		42,339 – 43,389	1.4	***42,700***	3,524 – 3,718	2.7	***3,616***
FRP-0.23		32,299 – 37,793	8.4	***34,500***	2,959 – 3,513	14.2	***2,918***

–Note: 791 °C-d averages for E_{469} and C_{469} include 2 specimens each. All other curing averages include 3 E_{469} and 3 C_{469}.

3.2.2 Curing assessment of cores and laboratory molded specimens

The 3- by 6-in. UHPC cores that were tested for compressive strength were used as a general curing reference relative to the four laboratory protocols utilized herein. These three cores produced an average compressive strength of 157 MPa and an average E_{469} of 55,900 MPa. These values were benchmarked with UHPC laboratory cast material into 3- by 6-in. cylinders that were reported earlier in this section. The range of average compressive strength and E_{469} were 149 to 190 MPa and 48,300 to 57,600, respectively.

The 3- by 6-in. UHPC cores that were tested for tensile strength were used as a general curing reference relative to the four laboratory protocols utilized herein. These six cores produced an average tensile strength of 19.8 MPa. These values were benchmarked with UHPC laboratory cast material into 3- by 6-in. cylinders that were reported earlier in this section. The range of average tensile strength was 20.8 to 24.4 MPa.

Variability was compared for the two available sets of UHPC tensile strength data cured in different manners where six replicates were available for 3- by 6-in. specimens. The 2,783 °C-d cured specimens had a COV of 20.6 percent. Cores had a COV of 17.3 percent.

3.3 Size effects

Of the 254 specimens produced, 69 were used to assess specimen size effects on measured properties of UHPC, CP-0.15, and FRP-0.23. The data contained in this section are sporadic. The best available information was collected herein with materials and resources remaining after proportions and curing effects were assessed. The effects of size on UHPC were found by comparing cores of two different diameters to laboratory cast specimens of a given diameter. The effects of size on CP-0.15 and FRP-0.23 were found by comparing lab made specimens of two different diameters that were identically cured. Some of the data utilized in this section were also used in Sections 3.1 or 3.2.

A general rule for producing specimens containing fibers is that the specimens' diameter must be at least three times the fiber length. For the fibers used in this project, that equates to 4- by 8-in. cylinders. Since 3- by 6-in. cylinders were mostly used herein to facilitate comparable testing with a range of constituents, 4- by 8-in. cylinders were made with fibers for comparative purposes. With regard to CP, most work to date in this area has used 2- by 4-in. specimens. Since 3- by 6-in. cylinders were mostly used herein to facilitate comparable testing with a range of constituents, 2- by 4-in. cylinders were made with CP for comparative purposes. In most cases, the compared cylinders were produced from the same batch for direct comparison.

3.3.1 Size effects – Ultra-High Performance Concrete (UHPC)

Minimal size effects data were collected for UHPC. The only assessment available was comparing 3- by 6-in. cores to 4- by 8-in. cores where the cores were taken from the same tub. As such, fiber orientation was established prior to coring and was comparable in both specimen sizes. The six cores that were 3- by 6-in. had an average tensile strength of 19.8 MPa, while the three cores that were 4- by 8-in. had an average tensile strength of 17.0 MPa.

3.3.2 Size effects – Cement paste (CP)

CP size effects data are summarized in Table 10, while Figure 19 plots the 24 individual specimens tested for compressive strength. All specimens were cured to 2,783 °C-d in the 23 °C curing room.

Of the 24 specimens utilized, six were from Section 3.2 curing effects that are repeated here and referred to as non-paired, since they were not made in the same batch as different sized specimens. The remaining 18 specimens were produced in three batches (six specimens per batch), where one batch produced three specimens that were 2 by 4 in. and three more specimens that were 3 by 6 in. These specimens could be viewed as matched pairs.

The paired *t*-test was performed on the nine matched pairs that could be produced from batches 1 to 3. The measured compressive strengths for each batch and specimen size were sorted in ascending order to make the pairs. For example, the lowest compressive strength of a 2- by 4-in. specimen from batch 1 was paired with the lowest compressive strength from a 3- by 6-in. cylinder from batch 1. The comparison was whether the mean difference of these pairs was statistically different from 0 at a 5 percent level of significance. The *p*-value was 0.33, indicating the values were not significantly different. The average strength of the 3- by 6-in. specimens from batches 1 to 3 was 124 MPa, while the average strength of the 2- by 4-in. specimens was 119 MPa.

If all 3- by 6-in. specimens were averaged (non-pairs and batches 1 to 3), the average strength was 118 MPa, which is within 1 MPa of the 2- by 4-in. specimens. When all data were considered, the standard deviation of the 3- by 6-in. specimens was 17 MPa, while the standard deviation for the 2- by 4-in. specimens was 21 MPa. Overall, there were no obvious differences between strengths produced with 2- by 4-in. specimens and those produced with 3- by 6-in. specimens.

Table 10. Size effects on CP data.

Mix ID	Size	Batch	fc Range (MPa)	fc COV (%)	fc Avg. (MPa)	Density Range (g/cm³)	Density COV (%)	Density Avg. (g/cm³)
CP-0.15	3x6	Non-Paired	78.0 – 143.4	21.0	*108.7*	2.188 – 2.271	1.8	*2.232*
CP-0.15	2x4	1	94.6 – 144.0	20.7	*119.5*	2.241 – 2.246	0.1	*2.244*
CP-0.15	3x6	1	127.3 – 129.9	1.1	*128.4*	2.247 – 2.254	0.2	*2.250*
CP-0.15	2x4	2	121.6 – 143.8	9.3	*129.9*	2.270 – 2.295	0.6	*2.284*
CP-0.15	3x6	2	119.9 – 138.7	7.4	*130.5*	2.248 – 2.267	0.4	*2.256*
CP-0.15	2x4	3	84.7 – 131.9	22.4	*106.5*	2.251 – 2.263	0.3	*2.255*
CP-0.15	3x6	3	111.9 – 116.0	1.9	*114.4*	2.209 – 2.230	0.5	*2.222*

--Notes: non-paired specimens – 6 fc, 6 densities
Batches 1, 2, and 3 had 3 fc and 3 densities for each specimen size.

Figure 19. Compressive strength of CP-0.15 size variation specimens.

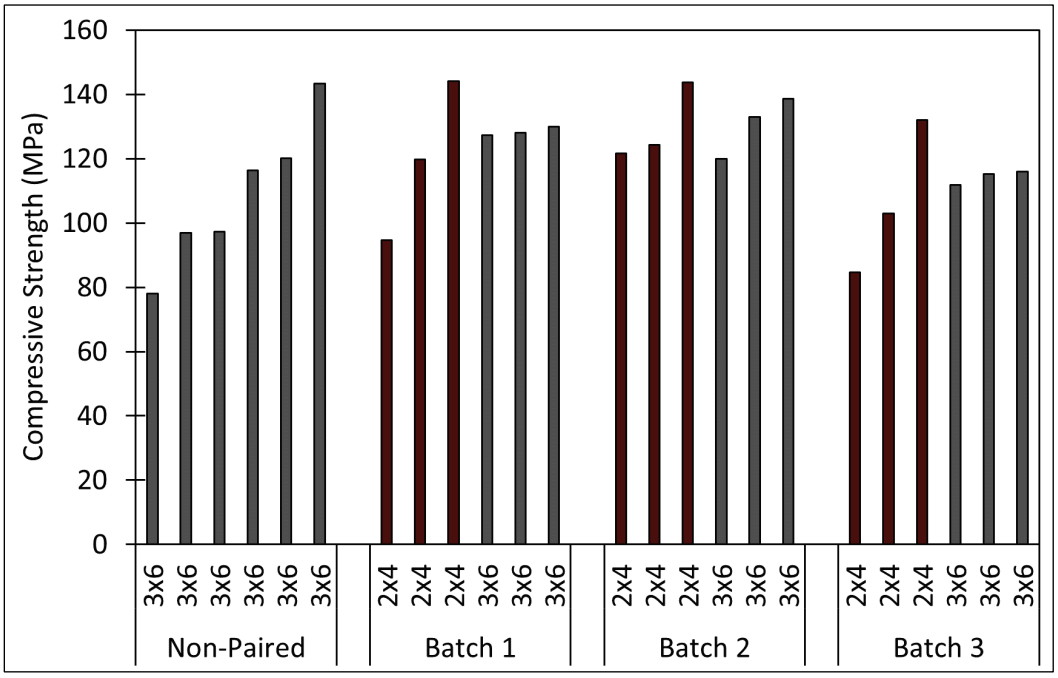

3.3.3 Size effects – Fiber Reinforced Paste (FRP)

FRP size effects data are summarized in Tables 11 (compression) and 12 (tension), while Figures 20 (compression) and 21 (tension) plot the 27 individual specimens tested. All specimens were cured to 2,783 °C-d in the 23 °C curing room.

Of the 27 specimens utilized, 12 were tested in compression, and 14 were tested in tension. In compression, six were non-paired (as described in

Section 3.3.2), and six were produced in two batches of three specimens each. Each batch produced two specimens that were 3 by 6 in. and one specimen that was 4 by 8 in. In tension, five were non-paired, and nine were produced in three batches of three specimens each. Each batch produced two specimens that were 3 by 6 in. and one specimen that was 4 by 8 in.

In compression, the 10 specimens that were 3 by 6 in. had an average compressive strength of 124 MPa with a range of 114 to 136 MPa. The two specimens that were 4 by 8 in. had strengths that were 119 and 135 MPa. Two observations can be made from these data, which are shown in Table 11 and Figure 20. First, the 4- by 8-in. specimens fell in the range of the 3- by 6-in. specimens. Second, for each batch from which multiple specimens were made, one of the 3- by 6-in. specimens was essentially the same as one of the 4- by 8-in. specimens.

Table 11. Size effects of FRP-0.23 in compression.

Mix ID	Size	Batch	fc Range (MPa)	fc COV (%)	fc Avg. (MPa)	Density Range (g/cm³)	Density COV (%)	Density Avg. (g/cm³)
FRP-0.23	3x6	Non-Paired	113.9 – 135.8	6.6	*122.2*	2.457 – 2.623	1.8	*2.531*
FRP-0.23	3x6	1	119.1 – 135.9	9.3	*127.5*	2.527 – 2.538	0.3	*2.532*
FRP-0.23	4x8	1	134.6	—	—	2.541	—	—
FRP-0.23	3x6	2	119.1 – 128.5	5.3	*123.8*	2.489 – 2.512	0.6	*2.500*
FRP-0.23	4x8	2	118.9	—	—	2.560	—	—

–Note: non-paired specimens – 6 fc, 6 densities
3x6 batched specimens – 2 fc, 2 densities
4x8 batched specimens – 1 fc, 1 density

Figure 20. Compressive strength of FRP variation specimens.

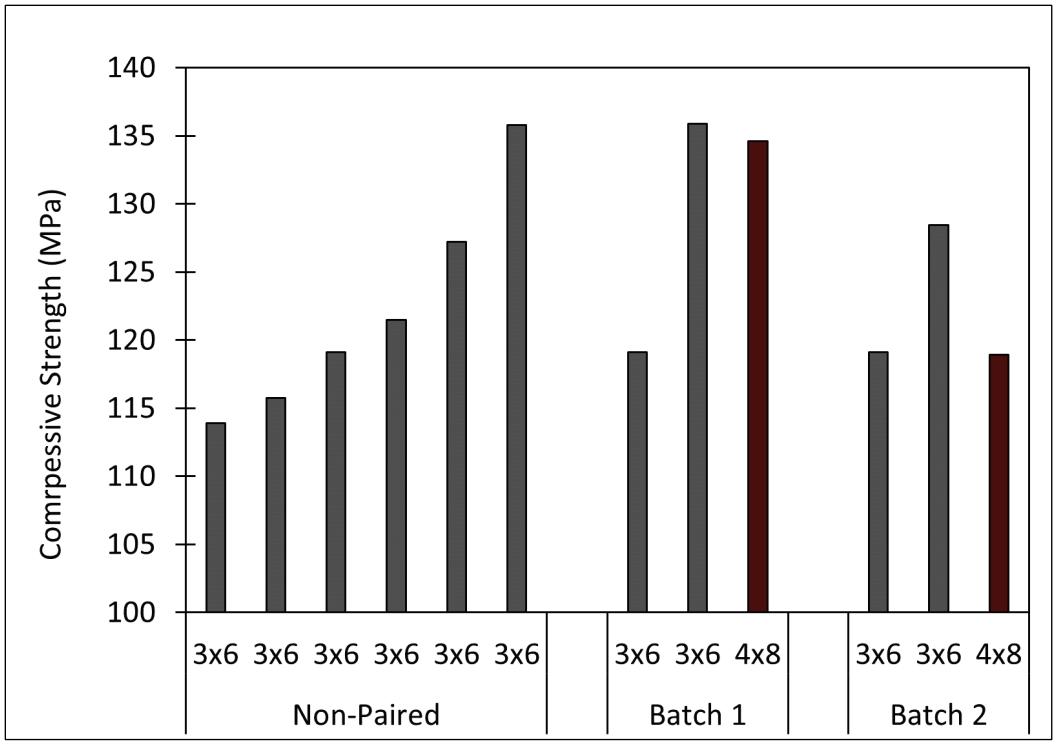

In tension, the 11 specimens that were 3 by 6 in. had an average tensile strength of 22.2 MPa with a range of 17.7 to 27.6 MPa. The three specimens that were 4 by 8 in. had strengths that were 17.5, 18.4, and 20.4 MPa with an average value of 18.8 MPa. Three observations can be made from these data, which are shown in Table 12 and Figure 21. First, the 4- by 8-in. specimens fell on the lower end of, to slightly below, the 3- by 6-in. specimens' range. Second, the average strength of 4- by 8-in. specimens was 85 percent of that from the 3- by 6-in. specimens. Third, the 4- by 8-in. specimen always had the lowest tensile strength in a given batch.

Table 12. Size effects on FRP-0.23 in tension.

Mix ID	Size	Batch	St Range (MPa)	St COV (%)	St Avg. (MPa)	Density Range (g/cm³)	Density COV (%)	Density Avg. (g/cm³)
FRP-0.23	3x6	Non-Paired	17.7 – 27.7	17.8	***22.0***	2.457 – 2.545	1.3	***2.511***
FRP-0.23	3x6	3	20.0 – 22.9	9.8	***21.5***	2.485 – 2.519	1.0	***2.502***
FRP-0.23	4x8	3	17.5	—	—	2.560	—	—
FRP-0.23	3x6	4	21.9 – 22.6	2.2	***22.2***	2.497 – 2.513	0.5	***2.505***
FRP-0.23	4x8	4	20.4	—	—	2.565	—	—
FRP-0.23	3x6	5	22.3 – 25.0	8.0	***23.6***	2.519 – 2.545	0.7	***2.532***
FRP-0.23	4x8	5	18.4	—	—	2.567	—	—

–Note: non-paired specimens – 5 st, 5 densities
3x6 batched specimens – 2 st, 2 densities
4x8 batched specimens – 1 st, 1 density

Figure 21. Tensile strength of FRP variation specimens.

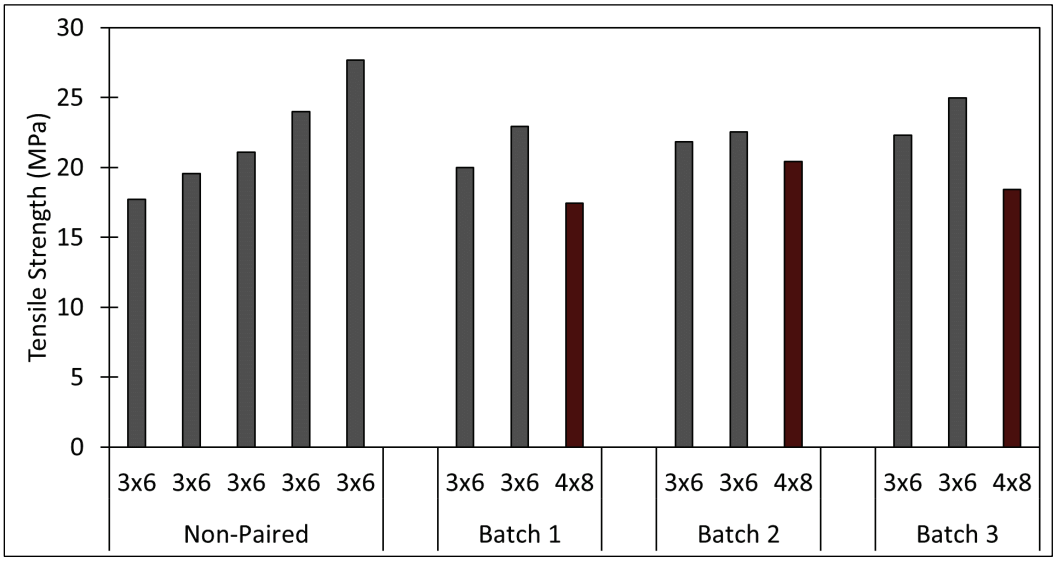

3.4 Instrumentation test results

Of the 254 specimens produced, eight were instrumented with strain gages after 791 °C-d curing. Each specimen was fitted with four strain gages, as shown in Appendix A. Of the 32 total strain gages, 27 measured data successfully. As noted earlier in the report, strain readings were taken with a data acquisition system independent of the concrete compression machine: load versus time was measured with the compression machine, and strain versus time was measured with the data acquisition system. These two time scales were synchronized within, at most, a few seconds so that stress versus

strain plots could be generated. The synchronization process was approximate but was reasonable for the purposes of this report.

In compression UHPC, CP-0.15, M-0.56, and FRP-0.23 were produced without replication where three strain gages were oriented vertically (parallel to axis of loading) and one gage was oriented horizontally. Figure 22 plots all strain readings taken in compression relative to the specimen's compressive strength (fc), which was determined by taking the stress at any instant in time, dividing by fc, and converting to a percentage. Strain readings were plotted for all gages up to 100 percent, and thereafter the curves were visually examined. Stress versus strain plots were truncated when visual evidence showed gage failure (e.g., a 1,000 microstrain change in strain from one reading to the next is likely gage debonding and not specimen response).

In tension UHPC, CP-0.15, M-0.56, and FRP-0.23 were produced without replication where three strain gages were oriented horizontally (perpendicular to axis of loading) and one gage was oriented vertically. Figure 23 plots strain readings relative to the specimen's tensile strength (St) in the same manner as Figure 22.

Figure 22. Percent of ultimate compressive stress versus strain for (a) UHPC, (b) CP-0.15, (c) M-0.56, and (d) FRP-0.23.

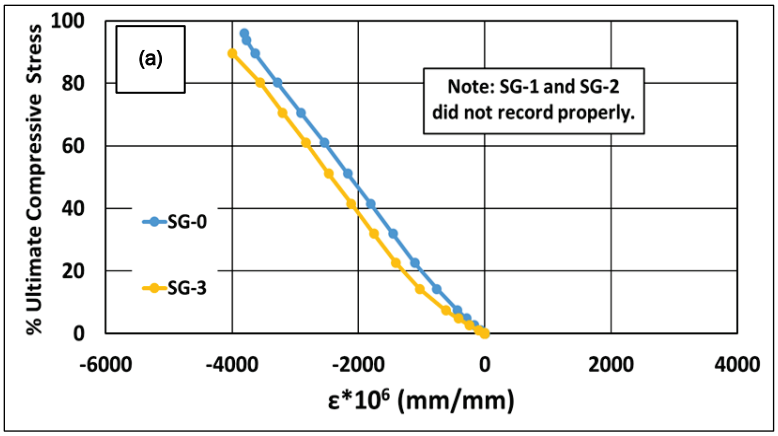

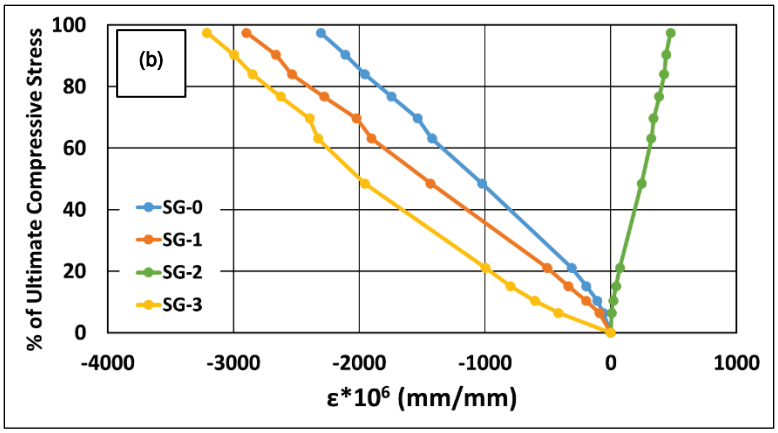
(b)
% of Ultimate Compressive Stress
100
80
60
40
20
0
SG-0
SG-1
SG-2
SG-3
-4000
-3000
-2000
-1000
0
1000
ε*10⁶ (mm/mm)

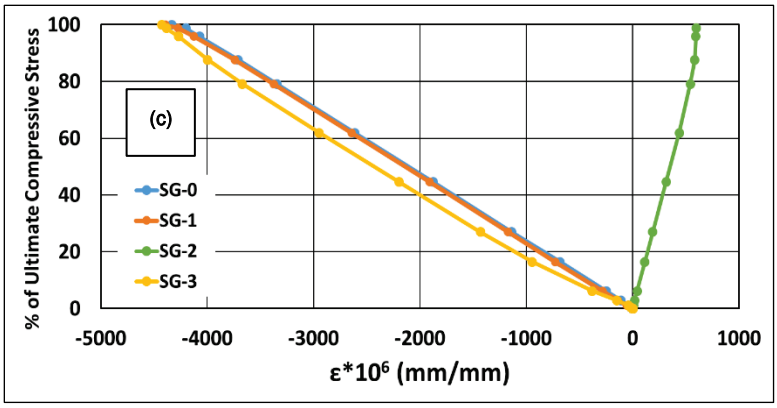
(c)
% of Ultimate Compressive Stress
100
80
60
40
20
0
SG-0
SG-1
SG-2
SG-3
-5000
-4000
-3000
-2000
-1000
0
1000
ε*10⁶ (mm/mm)

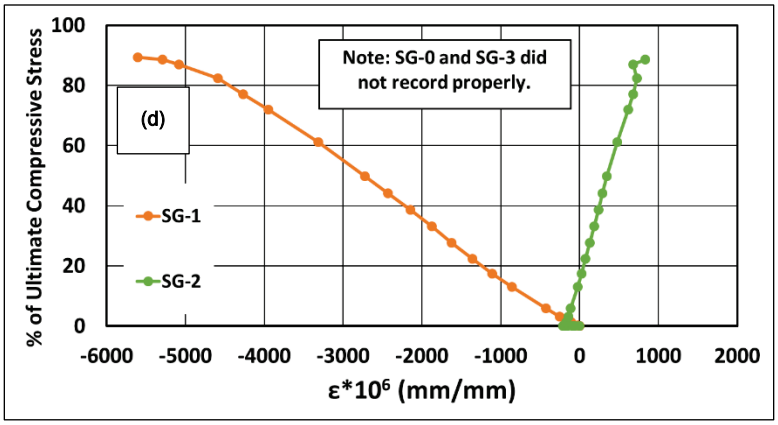
Note: SG-0 and SG-3 did not record properly.
(d)
% of Ultimate Compressive Stress
100
80
60
40
20
0
SG-1
SG-2
-6000
-5000
-4000
-3000
-2000
-1000
0
1000
2000
ε*10⁶ (mm/mm)

Figure 23. Percent of ultimate tensile stress versus strain for (a) UHPC, (b) CP-0.15, (c) M-0.56, and (d) FRP-0.23.

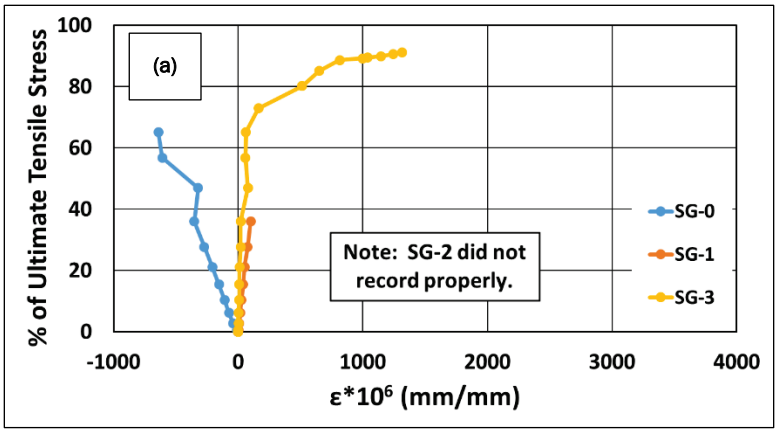

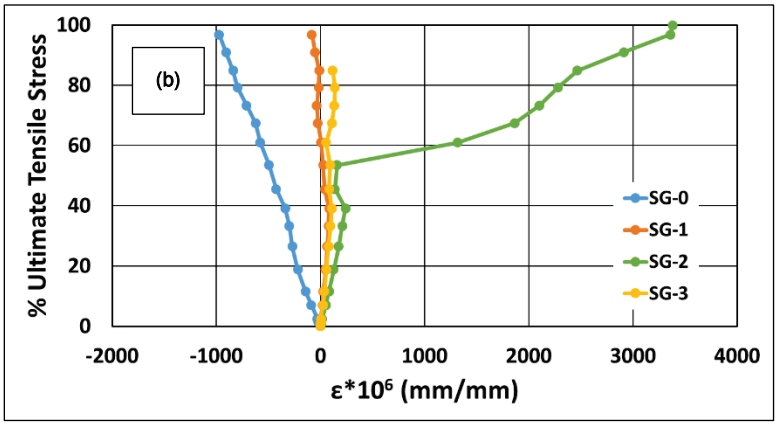

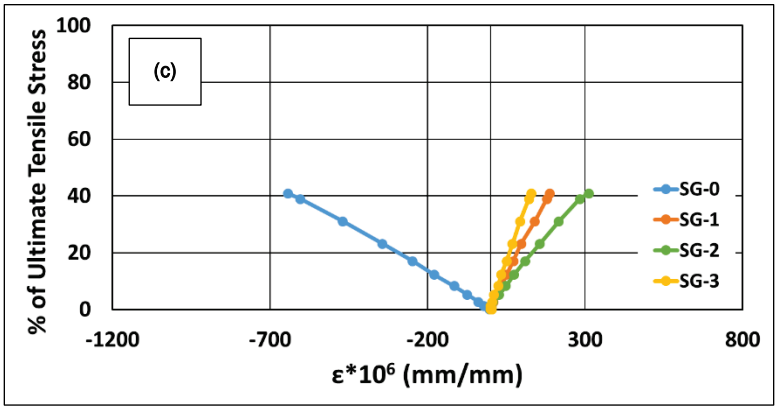

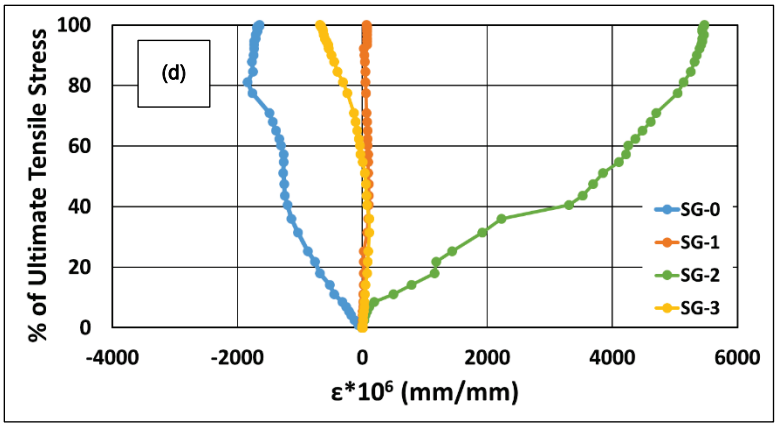

Numerical modeling of UHPC (or any of its constituents) benefits from knowing how high stresses can get before material behavioral changes are documented. When unconfined and tested as modest load rates, concrete materials are generally linear in their stress-strain behavior. A question, though, is how high can stresses get and linearity remain? As seen in Figures 22 and 23, linearity was often maintained at stresses nearing ultimate values, especially in compression. In tension, behaviors were somewhat more erratic.

Table 13 summarizes the highest ultimate tensile or compressive strain (ε_{max}) recorded by each gage in Figures 22 and 23 that was deemed reasonable from the aforementioned truncation process. Alongside this strain value is the percent of ultimate stress (%UltS) where this strain was recorded. For compressive loadings, linear behavior until 90 percent or more of %UltS was generally observed. Note that sampling rates were relatively low, and no useful information was collected as specimens approached failure.

Table 13. Strain gage data for compression and tension.

		SG-0		SG-1		SG-2		SG-3	
Mix	Mode	ε_{max}	%UltS	ε_{max}	%UltS	ε_{max}	%UltS	ε_{max}	%UltS
UHPC	Compression	-3,807	96%	—	—	—	—	-3,996	90%
	tension	-973	97%	-83	97%	3,381	100%	117	85%
CP-0.15	Compression	-2,307	98%	-2,897	98%	475	98%	-3,210	98%
	tension	-639	65%	100	36%	—	—	1,315	91%
M-0.56	Compression	-4,331	100%	-4,393	100%	600	99%	-4,426	100%
	tension	-644	41%	188	41%	311	41%	129	41%
FRP-0.23	Compression	—	—	-5,604	89%	831	89%	—	—
	tension	-1,649	100%	63	100%	5,472	100%	-678	100%

The linear portions of Figure 22 (vertical gages only) were used to produce stress-strain plots up to approximately 40 percent of ultimate stress for elastic modulus determination (Figure 24); elastic moduli calculated from strain gage measurements were denoted E_{SG-0} to E_{SG-3}. The ASTM C469 (ASTM International 2014) compressometer was also fitted to these same specimens to measure E_{469} so a direct comparison of strain gage and compressometer values could be made on the same specimen. Results are summarized in Table 14.

Figure 24. Truncated stress versus vertical strain plots for (a) UHPC, (b) CP-0.15, (c) M-0.56, and (d) FRP-0.23 in compression.

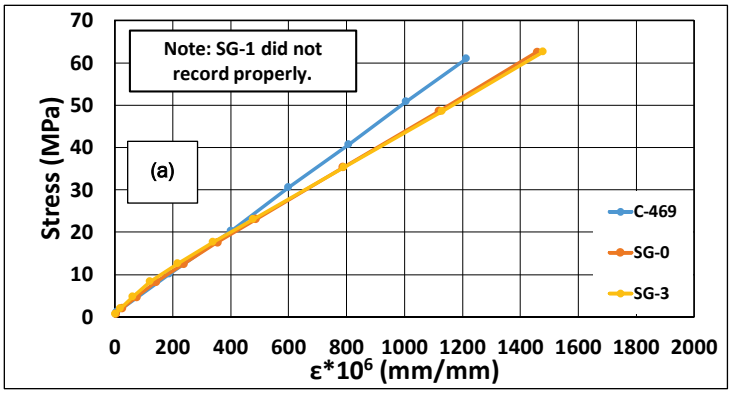

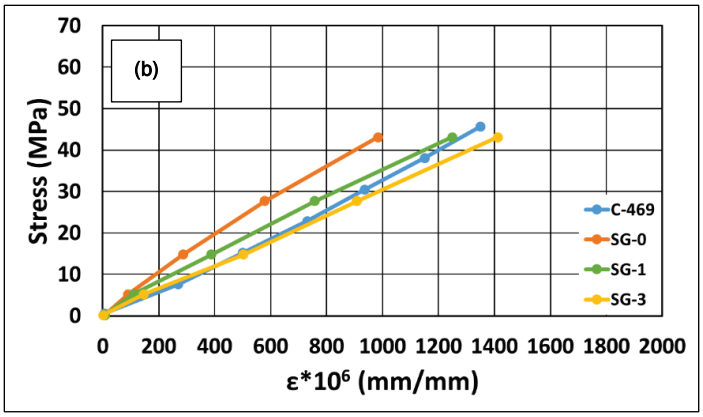

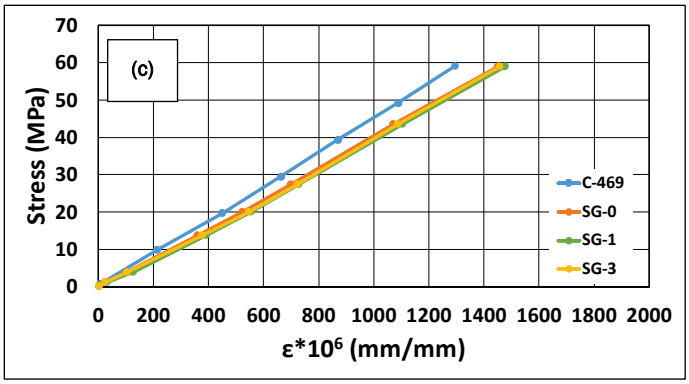

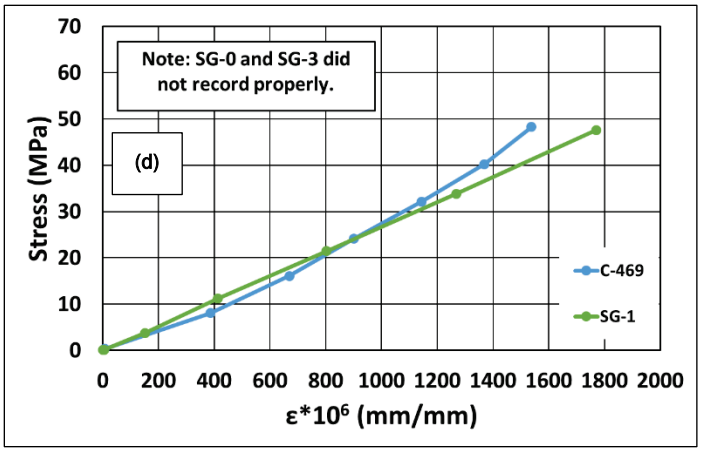

Table 14. Comparison of elastic moduli from strain gages and compressometer.

Mix ID	E_{SG-0} (MPa)	E_{SG-1} (MPa)	E_{SG-3} (MPa)	E_{SG-AVG} (MPa)	E_{469} (MPa)
UHPC	42,100	—	41,100	41,600	49,610
CP-0.15	43,700	34,200	30,300	36,000	33,800
M-0.56	40,700	40,000	40,300	40,300	45,300
FRP-0.23	—	26,800	—	26,800	31,400

--Note: All measurements shown in a given row were made on the same specimen.

In three cases, E469 resulted in higher values than strain gages (12 to 19 percent higher on average), and in 1 case, E469 resulted in lower values than strain gages (7 percent lower on average). Overall, strain gages and the compressometer reported elastic modulus values that were in the same general range based on this fairly limited data set.

From compression testing with strain gages, Poisson's ratio (υ) was approximated by relating the horizontal and vertical displacement using SG-2 (horizontally oriented) and SG-1 (vertically oriented). Figure 25 provides the plots used, which are truncations of Figure 22, and the corresponding Poisson's ratio values.

Figure 25. Poisson's ratio results from compression testing.

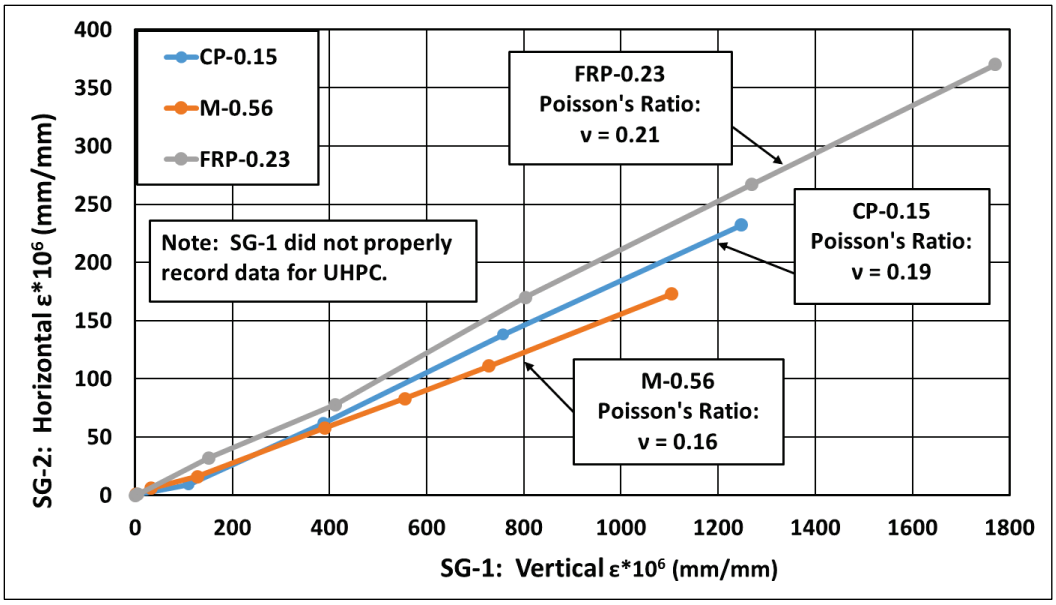

3.5 Volume fractions estimated from batch quantities

Table 15 shows the results of the volume fraction estimates from batch quantities and specific gravities of individual ingredients. All specimens tested except for cores are represented in Table 15. These fractions are approximations used for general reference and for comparison with the ImageJ and Abaqus results presented in the following section.

Table 15. Average volume fractions estimated from batch quantities.

Mix	V_c (%)	V_{sf} (%)	V_{sfl} (%)	V_s (%)	V_W (%)	V_f (%)	V_{am} (%)	V_a (%)	V_{TOTAL} (%)
UHPC	25.3	13.8	8.3	29.1	16.7	3.2	1.3	2.4	100
CP-0.15	44.0	24.0	-----	-----	29.0	-----	2.2	0.7	100
M-0.56	30.2	16.5	9.9	18.2	19.8	-----	1.5	3.9	100
FRP-0.11	41.7	22.7	-----	-----	27.5	5.2	2.1	0.9	100
CP-0.11	46.0	25.1	-----	-----	22.8	-----	2.3	3.8	100
CP-0.26	41.3	22.6	-----	-----	34.1	-----	2.1	0.01	100
M-0.47	31.5	17.2	10.4	14.3	20.8	-----	1.6	4.2	100
M-0.65	28.5	15.6	9.4	21.5	18.8	-----	1.4	4.8	100
FRP-0.17	42.4	23.2	-----	-----	28.0	4.0	2.1	0.3	100
FRP-0.23	42.7	23.3	-----	-----	28.2	2.7	2.1	1.0	100

3.6 Volume fractions estimated from imaging

Of the 254 specimens produced, five specimens (all cured for 791 °C-d) were allocated for image testing. Four of these specimens (UHPC, CP-0.15, M-0.56, and FRP-0.23) underwent imaging with an SEM that resulted in two dimensional (2-D) pictures, and the fifth specimen (UHPC) underwent a CT scan to get a 3-D representation of the UHPC.

Area fractions for the UHPC specimen evaluated with SEM techniques were found using ImageJ software. Table 16 compares the volume fractions in Table 15 to ImageJ values. It is important to note that the area fraction of cement found through imaging should not match the batching volume fraction. ImageJ found unhydrated cement grains, while the batching measures all cement put into the mixture.

One specimen also underwent a CT scan (Figure 26). Large voids, which can occur during mixing, were observed. Fiber orientation was assumed to be random, but the CT scan aided in observing the locations of the fibers within the matrix. The scan found that fibers were 3 percent of the total volume, which is close to what was calculated from batch quantities and found using imaging area.

Table 16. Comparison of average UHPC volume fractions from batching and ImageJ.

Inclusion	Estimated from batching quantities (%)	ImageJ (%)
Air voids	2.4	6.8
Cement	25.3	11.7
Sand	29.1	22.3
Fibers	3.2	3.7

Figure 26. CT scan of UHPC showing (a) approximately 3% steel fibers and (b) large voids illustrated.

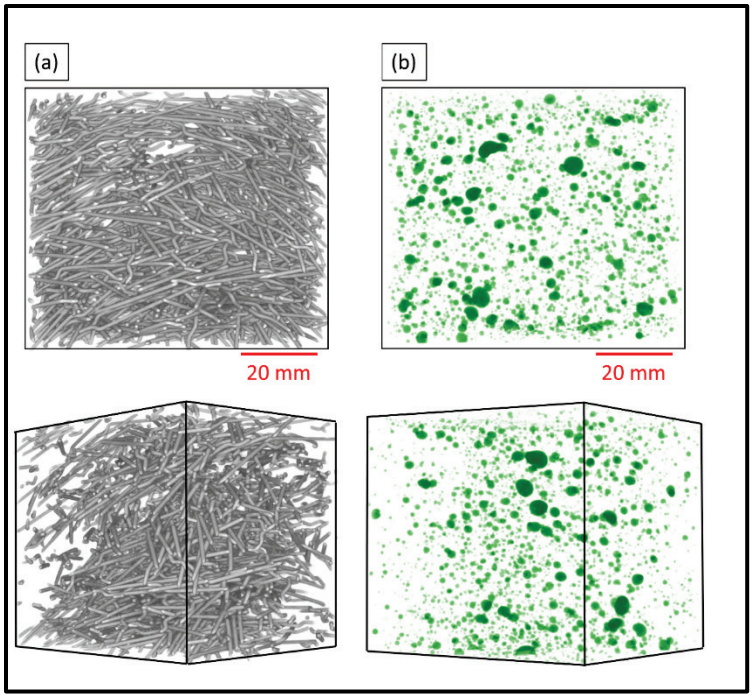

4 Summary

In simple terms, concrete properties are governed by aggregate properties, paste properties, and the bond between paste and aggregates when constituent materials and proportions are constant. However, understanding the true nature of how concrete properties are governed by these items is much more complex (even for constant materials). To provide some fundamental data on Cor-Tuf UHPC, a series of fundamental experiments was performed and is documented in this report, the ultimate purpose of which is to further numerical modeling efforts.

Cor-Tuf has seven constituent ingredients that lead to eight volume fractions when air voids are included. Ten mixtures were produced by using varying amounts of these seven ingredients and were exposed to varying curing times and temperatures. These mixtures can be divided into UHPC (all seven ingredients), FRP (no aggregates), M (no fibers), and CP (no aggregates or fibers). Mechanical property testing at low load rates and without confinement measured compressive strength, tensile strength, elastic modulus, Poisson's ratio, and load versus strain relationships. The majority of the specimens produced were 3 in. in diameter and had a height of 6 in., since this is a mid-range size for the types of mixtures produced. Some specimens were 2 in. by 4 in. or 4 in. by 8 in. to assess size effects.

This report is intended primarily to document these experiments and contain the data collected, since a systematic evaluation of this nature related to constituent effects is not readily available to the knowledge of the authors. Specific conclusions are avoided herein as the intent is to use these data in future efforts that will be more appropriate to draw more meaningful conclusions about ways to better model and ultimately improve UHPC. An intended purpose for these data is high-performance computing (HPC) environments where multi-scale modeling is performed. Fundamental understanding of individual components, proportions, and their interface behavior is needed for sophisticated numerical models capable of predicting behavior of structural systems built with UHPC. The experimental data collected have the possibility to be used three ways for numerical modeling purposes: (1) exploratory efforts to assist in defining first principles, (2) calibration, and (3) validation.

The following list summarizes key observations from this report.

1. Instrumented compression specimens showed mostly linear behavior to stress levels of 90 percent (or more) of failure levels.
2. Specimens produced with UHPC constituent materials did not produce as high of an elastic modulus per unit of compressive strength as does typical ready mixed concrete.
3. With CP, there were no overall obvious compressive strength differences between 2- by 4-in. specimens and 3- by 6-in. specimens.
4. With FRP, compressive strengths from 4- by 8-in. specimens fell in the range of those from 3- by 6-in. specimens. Tensile strengths from 4- by 8-in. specimens fell on the lower end of to slightly lower than 3- by 6-in. specimens. Note that 4- by 8-in. specimen data were limited.
5. Specific aspects of curing seem to affect compressive and tensile properties, and the effects are not consistent between tension and compression or between types of specimen. These data suggest that only accumulating ^{o}C-days and using that number as a maturity index may lead to undesirable outcomes for some types of UHPC endeavors, such as mass concrete.

References

Abaqus CAE (version 6.14). 2014. Dassault Systems.

American Concrete Institute. 2014. Building code requirements for structural concrete (ACI 318-05) and commentary (ACI 318R-05). Farmington Hills, MI: American Concrete Institute.

American Petroleum Institute. 1991. Specification for well cements, API specification IOA. 21st ed. September, 1991. Washington DC: American Petroleum Institute.

ASTM International (ASTM). 2011a. *Standard practice for estimating concrete strength by the maturity method*. Designation C1074-11. West Conshohocken, PA: ASTM International. Doi: 10.1520/C1074-11. www.astm.org/

_____. 2011b. *Standard test method for splitting tensile strength of cylindrical concrete specimens*. Designation C496/C496M. West Conshohocken, PA: ASTM International. Doi 10.1520/C0496_C0496M-11. https://www.astm.org/

_____. 2013. *Standard specification for chemical admixtures for use in producing flowing concrete*. Designation C1017/C1017M-13E01. West Conshohocken, PA: ASTM International. Doi 10.1520/C1017_C 1017M-13E01. https://www.astm.org/

_____. 2014. *Standard test method for static modulus of elasticity and Poisson's ration of concrete in compression*. Designation: C469/C469M. West Conshohocken, PA: ASTM International. Doi: 10.1520/C0469M-14. https://www.astm.org/

_____. 2015. *Standard test methods for chemical analysis of hydraulic cement*. Designation: C114/C114M. West Conshohocken, PA: ASTM International. Doi: 10.1520/C0114-15. https://www.astm.org/

_____. 2016a. *Standard specification for steel fibers for fiber-reinforced concrete*. West Conshohocken, PA: ASTM International. Doi: 10.1520/A0820_A0820M-16. https://www.astm.org/

_____. 2016b. *Standard test method for compressive strength of cylindrical concrete specimens*. Designation: C39/C39M. West Conshohocken, PA: ASTM International. Doi: 10.1520/C0039_C0039M-16. https://www.astm.org/

_____. 2017a. *Standard specification for chemical admixtures for concrete*. Designation: C494/C494M. West Conshohocken, PA: ASTM International. Doi: 10.1520/C0494_C0494M-17. https://www.astm.org/

_____. 2017b. *Standard test methods for fineness of hydraulic cement by air-permeability apparatus*. Designation: C204/C204M. West Conshohocken, PA: ASTM International. Doi: 10.1520 C0204-17. https://www.astm.org/

Chandler, M., J. Peters, and D. Pelessone. 2012. *Modeling nanomechanical behavior of calcium-silicate-hydrate*. ERDC/GSL TR-12-30. Vicksburg, MS: U.S. Army Engineer and Research and Development Center.

Green, B., R. Moser, D. Scott, and W. Long. 2014. Ultra-high performance concrete history and usage by the Corps of Engineers. *Advances in Civil Engineering Materials* 4(2): 132-143. https://doi.org/10.1520/ACEM20140031.

Howard, I. L., and H. V. GangaRao. 2009. Testing and evaluation of adhesive bonded fiber reinforced polymer bridge decks. *Journal of Advanced Materials* 41(2): 28-46.

Roth, M. J. 2008. *Flexural and tensile properties of thin, very high-strength, fiber-reinforced concrete panels*. ERDC/GSL TR-08-24. Vicksburg, MS: U.S. Army Engineer Research and Development Center.

Rushing, T. W., I. L. Howard, J. B. Jordan, and P. G. Allison. 2016. Laboratory characterization of fatigue performance of AM2 aluminum airfield matting. *Journal of Materials in Civil Engineering* 28(11): 04016134.

Schneider, C. A., W. S. Rasband, and K. W. Eliceiri. 2012. NIH image to ImageJ: 25 years of image analysis. *Nature Methods* 9(7): 671–75.

Scott, D., W. Long, R. Moser, B. Green, J. O'Daniel, and B. Williams. 2015. *Impact of steel fiber size and shape on the mechanical properties of ultra-high performance concrete*. ERDC/GSL TR-15-22. Vicksburg, MS: U.S. Army Engineer Research and Development Center.

Warren, K. A., B. Christopher, and I. L. Howard. 2010. Geosynthetic strain gage installation procedures and alternative strain measurement methods for roadway applications. *Geosynthetics International* 17(6): 403-430.

Appendix A: Strain Gage Locations

Figure A1. Strain gage locations of UHPC in compression.

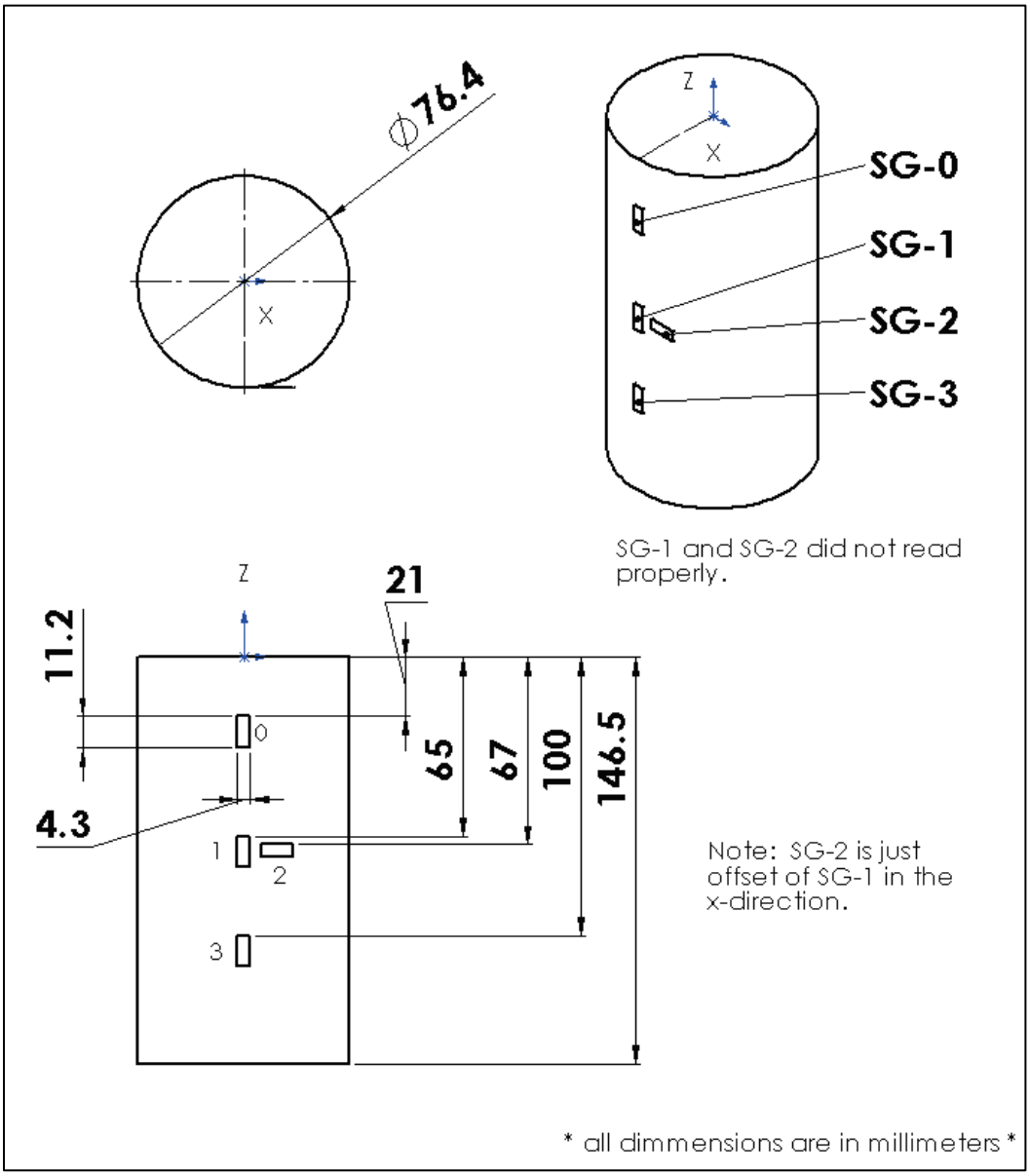

Figure A2. Strain gage locations for CP in compression.

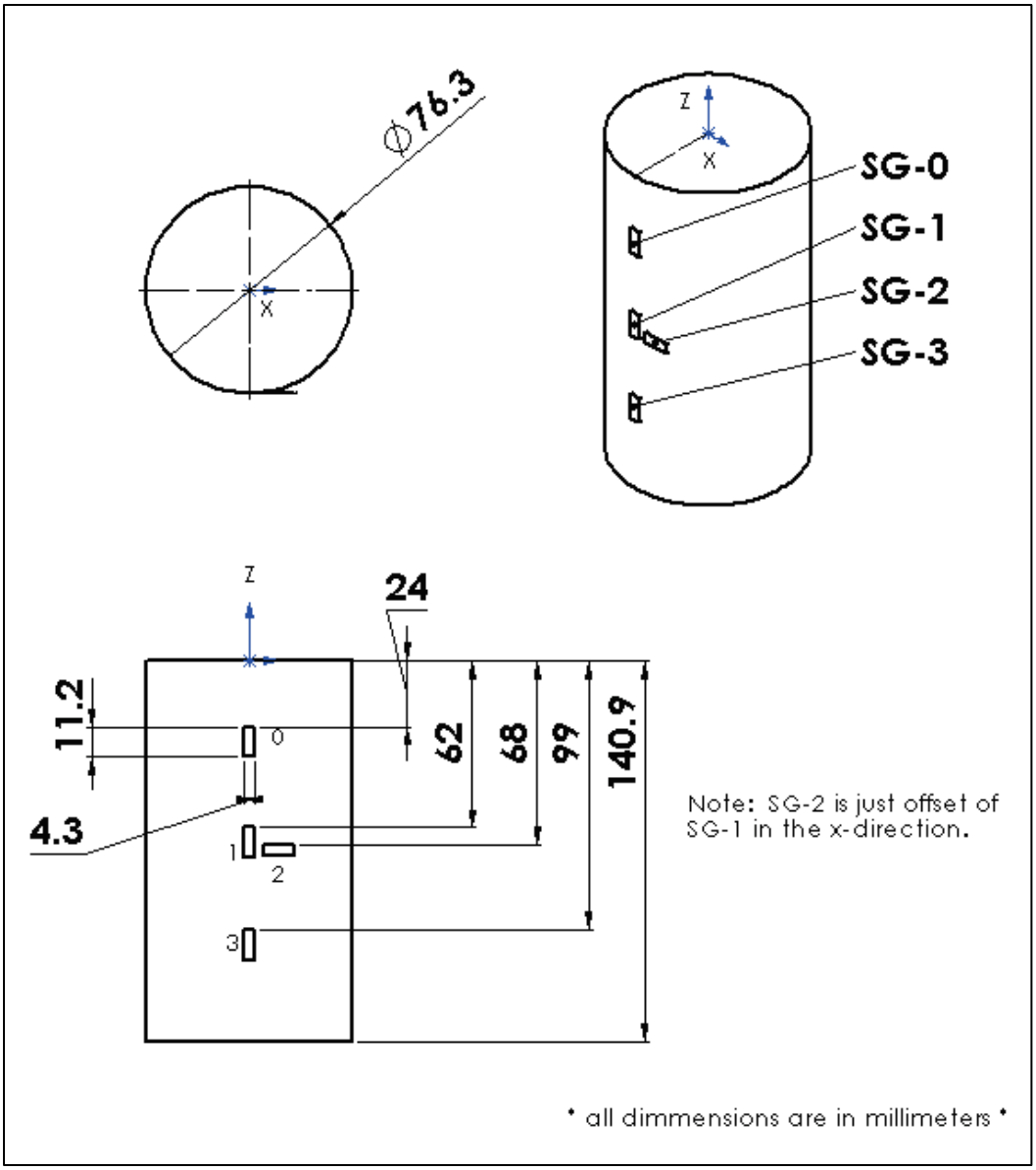

Figure A3. Strain gage locations for M in compression.

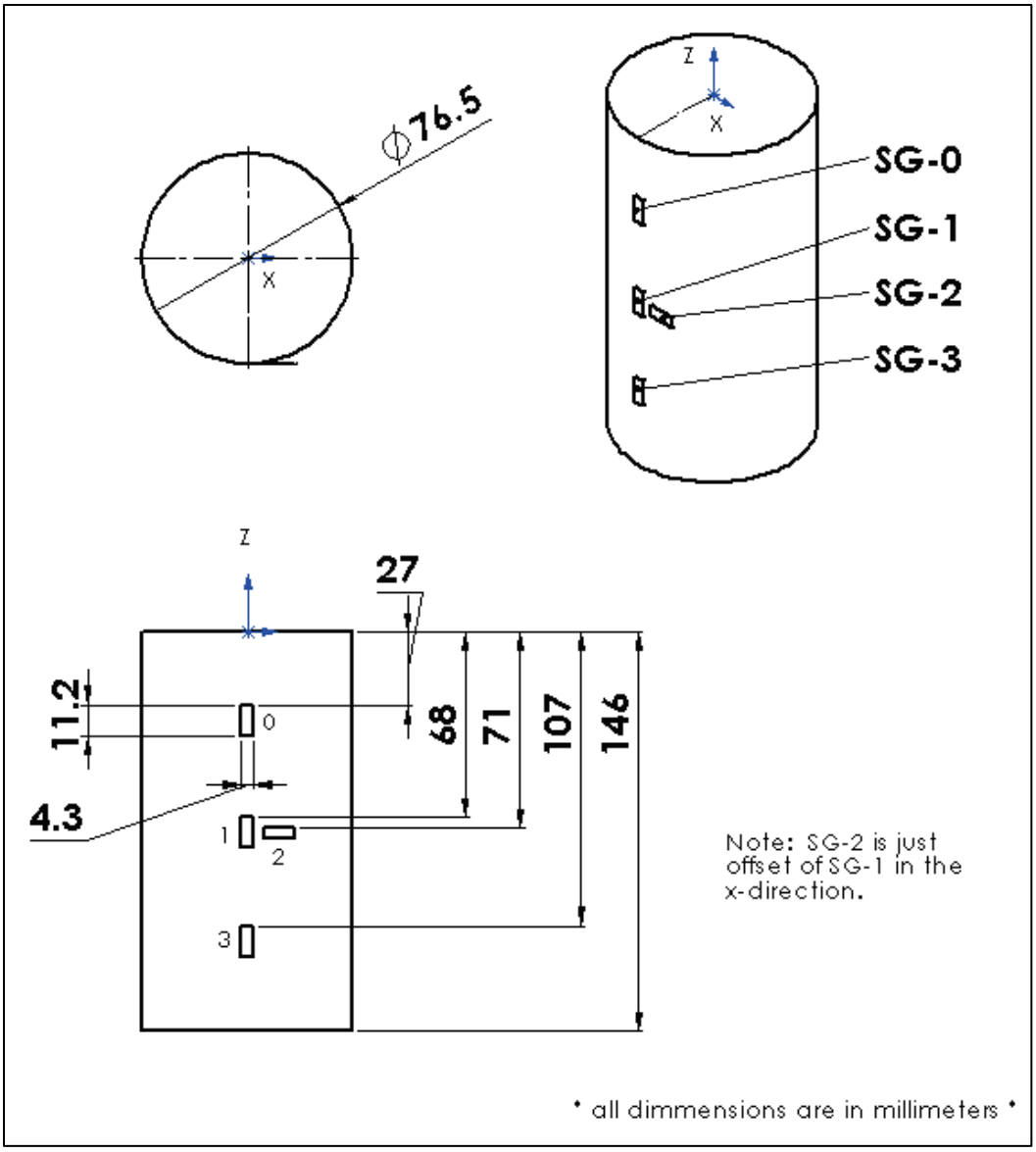

Figure A4. Strain gage locations for FRP in compression.

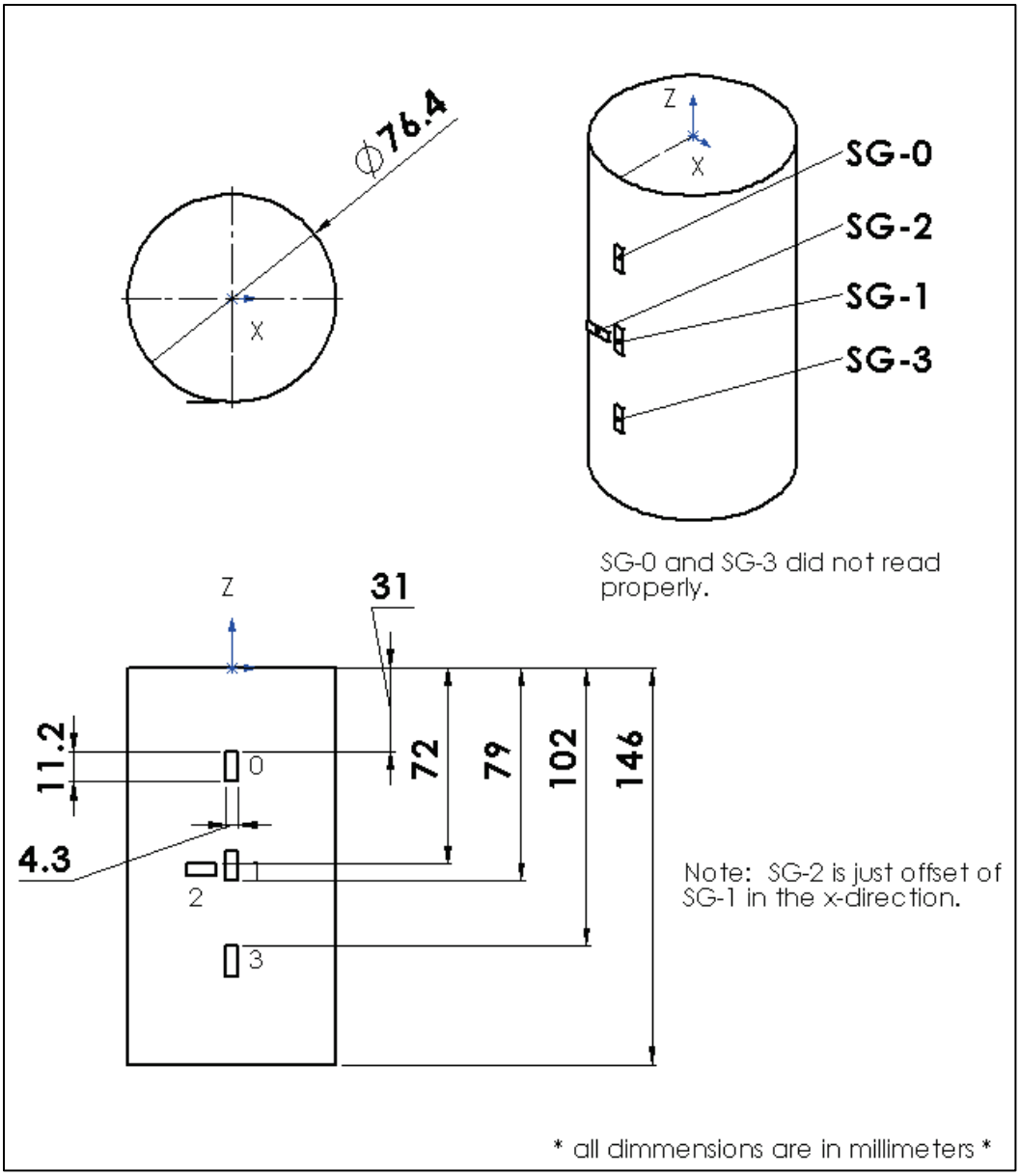

Figure A5. Strain gage locations for UHPC in tension.

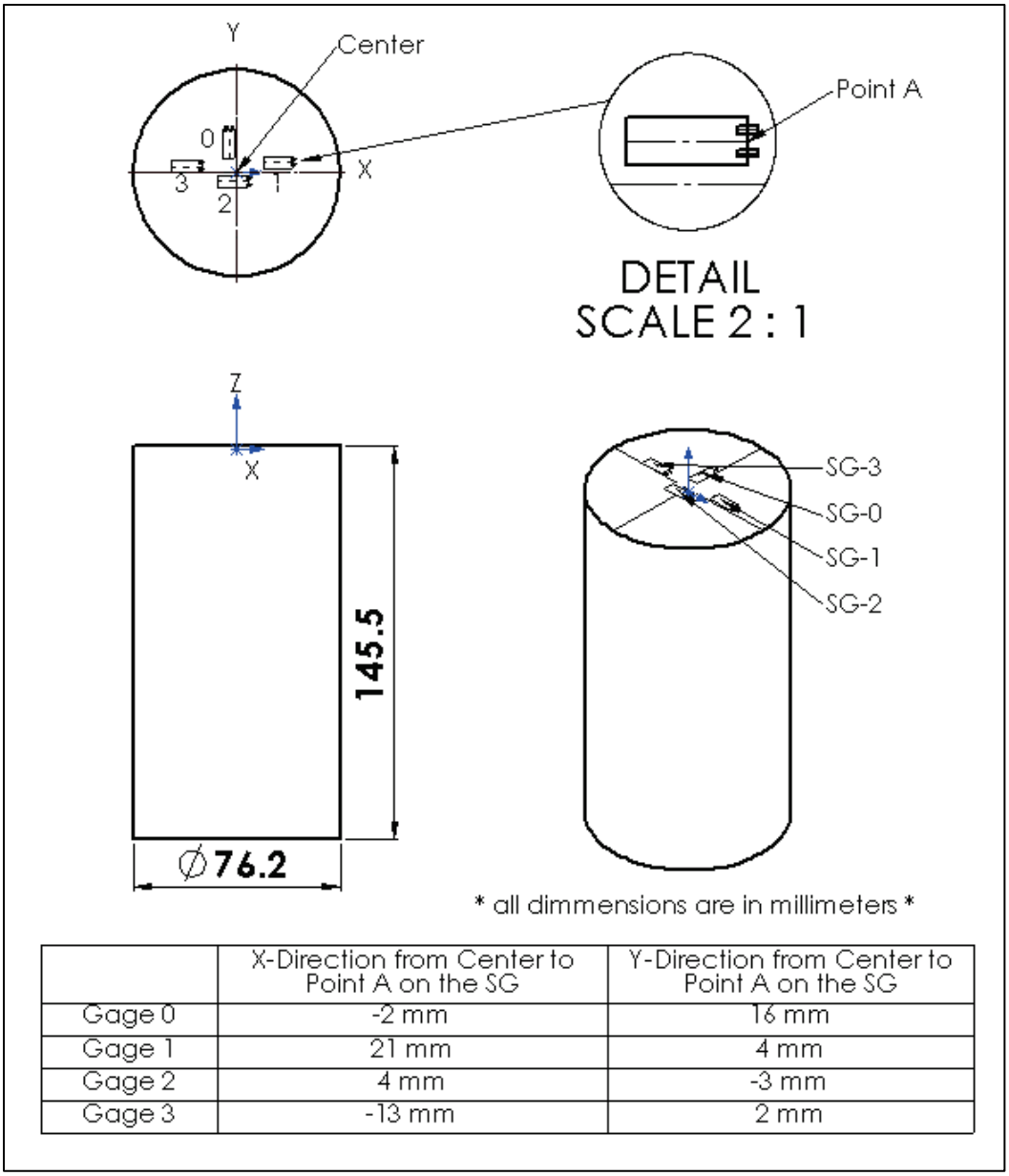

	X-Direction from Center to Point A on the SG	Y-Direction from Center to Point A on the SG
Gage 0	-2 mm	16 mm
Gage 1	21 mm	4 mm
Gage 2	4 mm	-3 mm
Gage 3	-13 mm	2 mm

Figure A6. Strain gage locations for CP in tension.

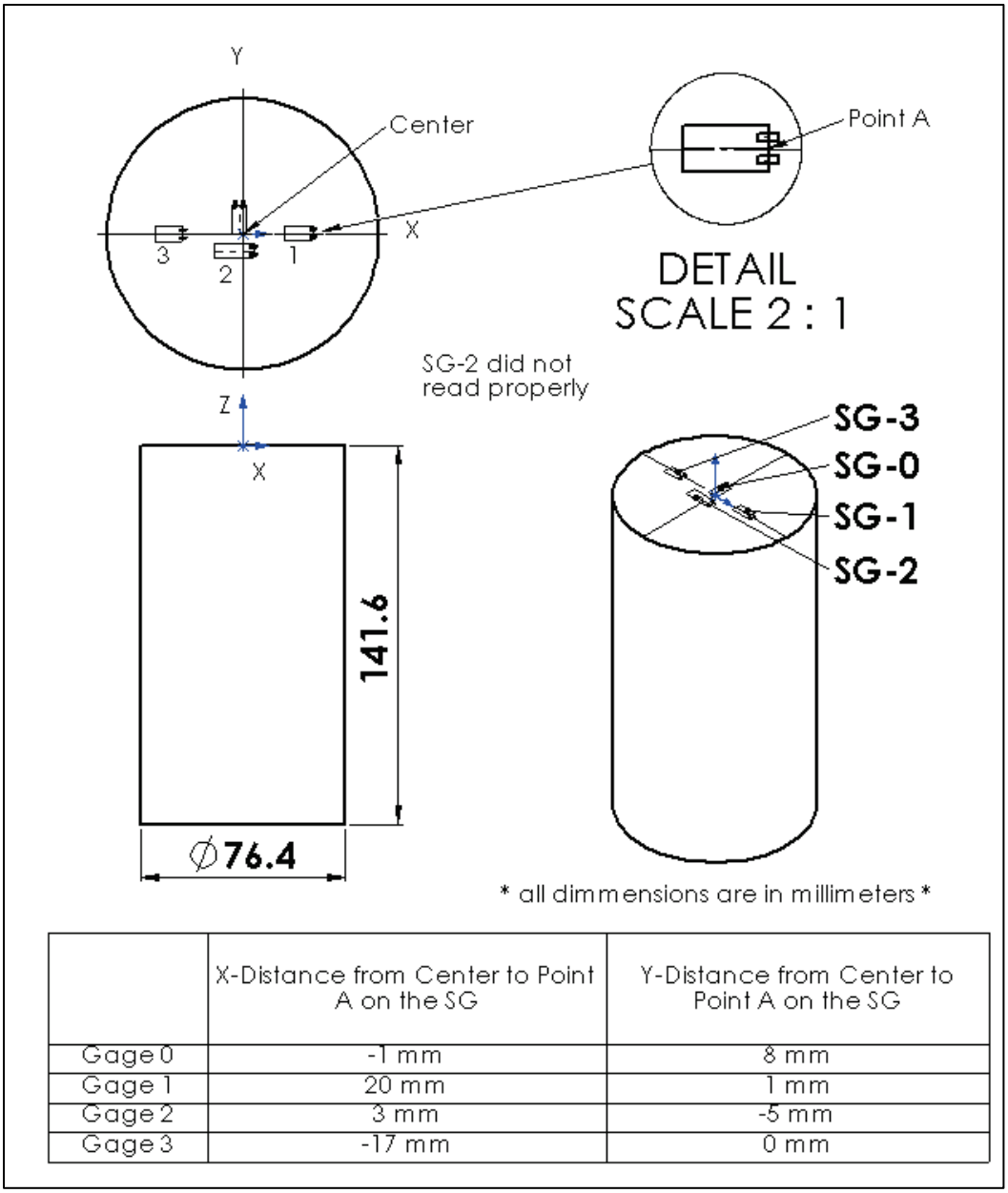

	X-Distance from Center to Point A on the SG	Y-Distance from Center to Point A on the SG
Gage 0	-1 mm	8 mm
Gage 1	20 mm	1 mm
Gage 2	3 mm	-5 mm
Gage 3	-17 mm	0 mm

Figure A7. Strain gage locations for M in tension.

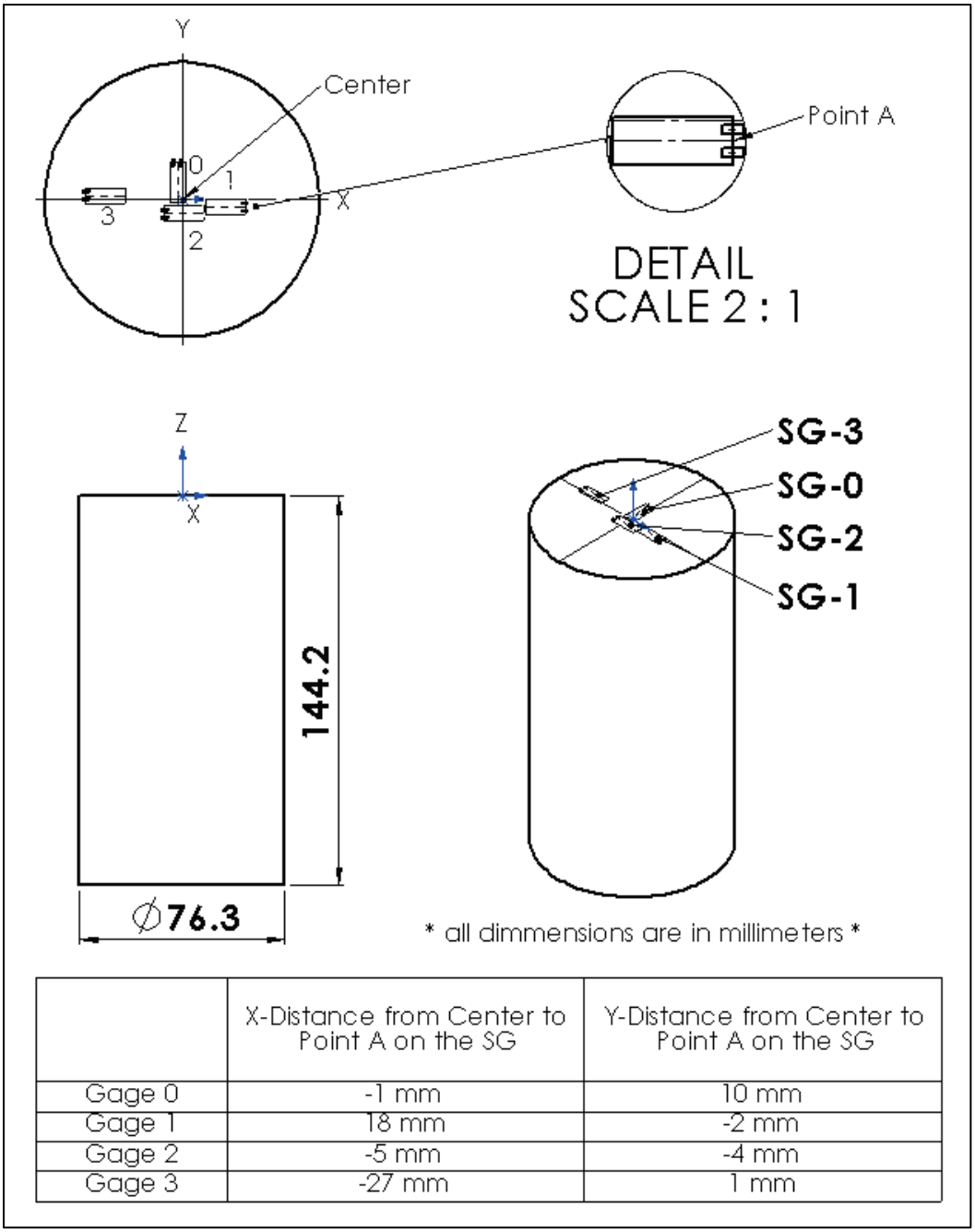

	X-Distance from Center to Point A on the SG	Y-Distance from Center to Point A on the SG
Gage 0	-1 mm	10 mm
Gage 1	18 mm	-2 mm
Gage 2	-5 mm	-4 mm
Gage 3	-27 mm	1 mm

Figure A8. Strain gage locations for FRP in tension.

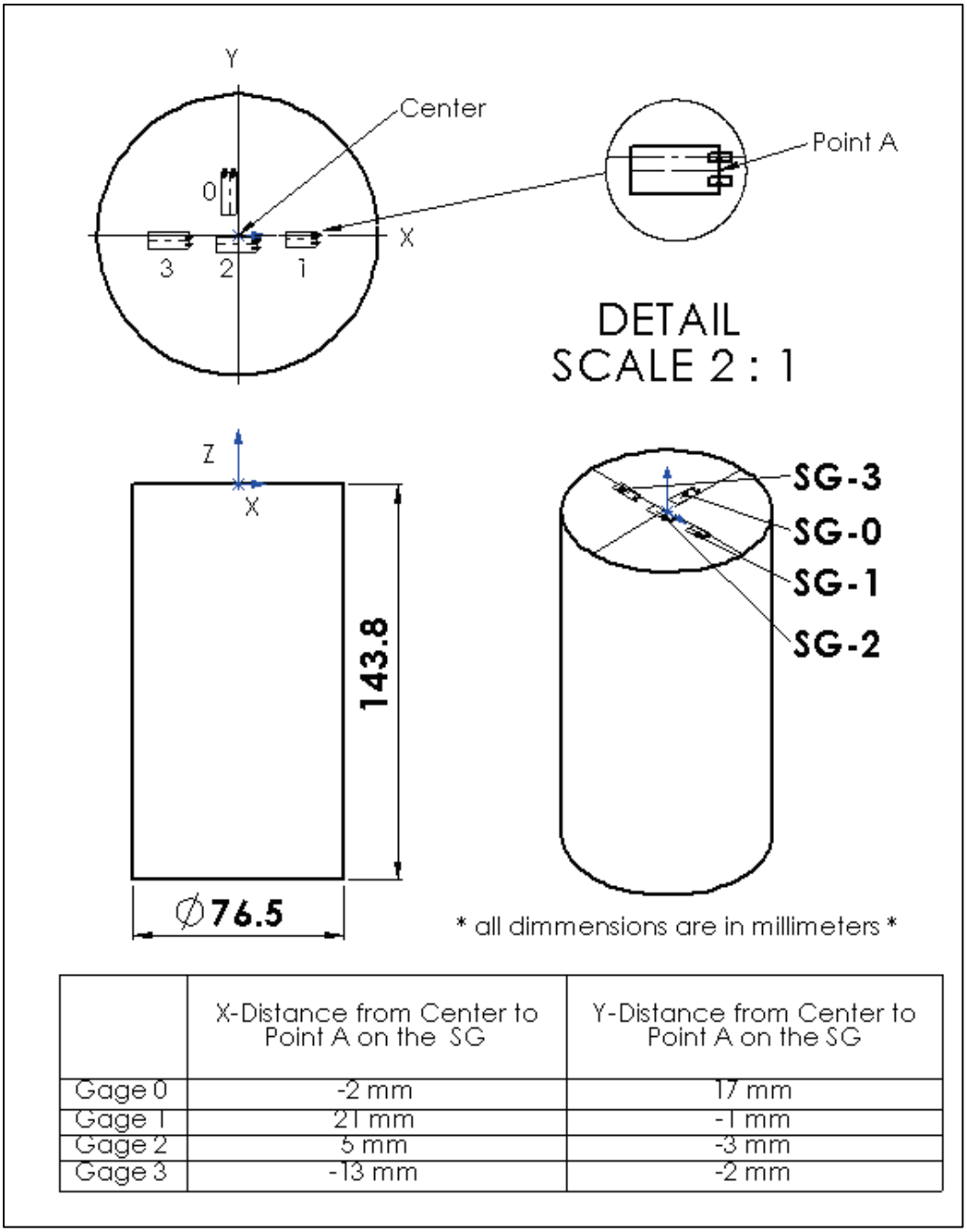

	X-Distance from Center to Point A on the SG	Y-Distance from Center to Point A on the SG
Gage 0	-2 mm	17 mm
Gage 1	21 mm	-1 mm
Gage 2	5 mm	-3 mm
Gage 3	-13 mm	-2 mm

REPORT DOCUMENTATION PAGE

Form Approved
OMB No. 0704-0188

Public reporting burden for this collection of information is estimated to average 1 hour per response, including the time for reviewing instructions, searching existing data sources, gathering and maintaining the data needed, and completing and reviewing this collection of information. Send comments regarding this burden estimate or any other aspect of this collection of information, including suggestions for reducing this burden to Department of Defense, Washington Headquarters Services, Directorate for Information Operations and Reports (0704-0188), 1215 Jefferson Davis Highway, Suite 1204, Arlington, VA 22202-4302. Respondents should be aware that notwithstanding any other provision of law, no person shall be subject to any penalty for failing to comply with a collection of information if it does not display a currently valid OMB control number. **PLEASE DO NOT RETURN YOUR FORM TO THE ABOVE ADDRESS.**

1. REPORT DATE *(DD-MM-YYYY)*	**2. REPORT TYPE**	**3. DATES COVERED** *(From - To)*
October 2018	Final report	

4. TITLE AND SUBTITLE
Mechanical Behavior of Cor-Tuf Ultra-High-Performance Concrete Considering Aggregate and Paste Effects

5a. CONTRACT NUMBER
W56HZV-17-C-0095

5b. GRANT NUMBER

5c. PROGRAM ELEMENT NUMBER

6. AUTHOR(S)
Isaac L. Howard, Ashley Carey, Megan Burcham, Dylan A. Scott, Jameson D. Shannon, Robert D. Moser, and Mark F. Horstemeyer

5d. PROJECT NUMBER
458161

5e. TASK NUMBER

5f. WORK UNIT NUMBER
J495LJ

7. PERFORMING ORGANIZATION NAME(S) AND ADDRESS(ES)

U.S. Army Engineer Research and Development Center
Geotechnical and Structures Laboratory
3909 Halls Ferry Road
Vicksburg, MS 39180-6199

8. PERFORMING ORGANIZATION REPORT NUMBER

ERDC/GSL TR-18-31

9. SPONSORING / MONITORING AGENCY NAME(S) AND ADDRESS(ES)
U.S. Army Corps of Engineers
Washington DC 20314-1000

10. SPONSOR/MONITOR'S ACRONYM(S)

11. SPONSOR/MONITOR'S REPORT NUMBER(S)

12. DISTRIBUTION / AVAILABILITY STATEMENT

Approved for public release; distribution is unlimited.

13. SUPPLEMENTARY NOTES

14. ABSTRACT
This research primarily focused on properties from varying the constituents that make up ultra-high performance concrete (UHPC) with the ultimate goal to enable improved characterization and modeling of this material. Several variations of UHPC were made to see the differences in properties as a function of constituents. Compressive strength, elastic modulus, and tensile strength were measured at low loading rates. Fundamental test methods were used for most experiments with a smaller subset of tests with strain gages and imaging techniques. This report is intended primarily to document these experiments and the collected data. Specific conclusions are avoided herein, as the intent is to use these data in future efforts that will be more appropriate to draw more meaningful conclusions about ways to better model and ultimately improve UHPC.

15. SUBJECT TERMS
UHPC, Cor-Tuf, Concrete-Mechanical properties, Characterization, microCT, Concrete-Mixing, Concrete-Additives, High strength concrete, Modeling, Concrete, Aggregates (Building materials)

16. SECURITY CLASSIFICATION OF:			**17. LIMITATION OF ABSTRACT**	**18. NUMBER OF PAGES**	**19a. NAME OF RESPONSIBLE PERSON** Robert D. Moser
a. REPORT	**b. ABSTRACT**	**c. THIS PAGE**			**19b. TELEPHONE NUMBER** *(include area code)*
UNCLASSIFIED	UNCLASSIFIED	UNCLASSIFIED		74	601.634.3261